Sedimentology (2006) **53,** 867–897 doi: 10.1111/j.1365-3091.2006.00797.x

Sea-level and tectonic control of middle to late Pleistocene turbidite systems in Santa Monica Basin, offshore California

WILLIAM R. NORMARK*, DAVID J. W. PIPER† and RAY SLITER*
**US Geological Survey, 345 Middlefield Road, Menlo Park, CA 94025, USA (E-mail: wnormark@usgs.gov)*
†Geological Survey of Canada (Atlantic), Bedford Institute of Oceanography, P.O. Box 1006, Dartmouth, Nova Scotia, B2Y 4A2, Canada

ABSTRACT

Small turbidite systems offshore from southern California provide an opportunity to track sediment from river source through the turbidity-current initiation process to ultimate deposition, and to evaluate the impact of changing sea level and tectonics. The Santa Monica Basin is almost a closed system for terrigenous sediment input, and is supplied principally from the Santa Clara River. The Hueneme fan is supplied directly by the river, whereas the smaller Mugu and Dume fans are nourished by southward longshore drift. This study of the Late Quaternary turbidite fill of the Santa Monica Basin uses a dense grid of high-resolution seismic-reflection profiles tied to new radiocarbon ages for Ocean Drilling Program (ODP) Site 1015 back to 32 ka. Over the last glacial cycle, sedimentation rates in the distal part of Santa Monica Basin averaged 2–3 mm yr^{-1}, with increases at times of extreme relative sea-level lowstand. Coarser-grained mid-fan lobes prograded into the basin from the Hueneme, Mugu and Dume fans at times of rapid sea-level fall. These pulses of coarse-grained sediment resulted from river channel incision and delta cannibalization. During the extreme lowstand of the last glacial maximum, sediment delivery was concentrated on the Hueneme Fan, with mean depositional rates of up to 13 mm yr^{-1} on the mid- and upper fan. During the marine isotope stage (MIS) 2 transgression, enhanced rates of sedimentation of > 4 mm yr^{-1} occurred on the Mugu and Dume fans, as a result of distributary switching and southward littoral drift providing nourishment to these fan systems. Longer-term sediment delivery to Santa Monica Basin was controlled by tectonics. Prior to MIS 10, the Anacapa ridge blocked the southward discharge of the Santa Clara River into the Santa Monica Basin. The pattern and distribution of turbidite sedimentation was strongly controlled by sea level through the rate of supply of coarse sediment and the style of initiation of turbidity currents. These two factors appear to have been more important than the absolute position of sea level.

Keywords Canyon, chronology, Quaternary, sea level, submarine fan, tectonics, turbidite.

INTRODUCTION

The Santa Monica Basin, including the Hueneme Fan, is one of the best known small sandy turbidite systems in the world (Fig. 1), as a result of detailed studies of Holocene sedimentation by Gorsline and his colleagues (Nardin, 1983; Reynolds, 1987; Christensen *et al.*, 1994; Gorsline, 1996; Schwalbach *et al.*, 1996) and interpretation of a suite of seismic-reflection profiles by the present authors (Normark *et al.*, 1998; Piper *et al.*, 1999; Piper & Normark, 2001). The Santa Monica Basin is a closed depositional system that receives sediment from the Santa Clara and Ventura rivers in the north and the Los Angeles Basin drainages in the south – short, high-sediment-load (dirty)

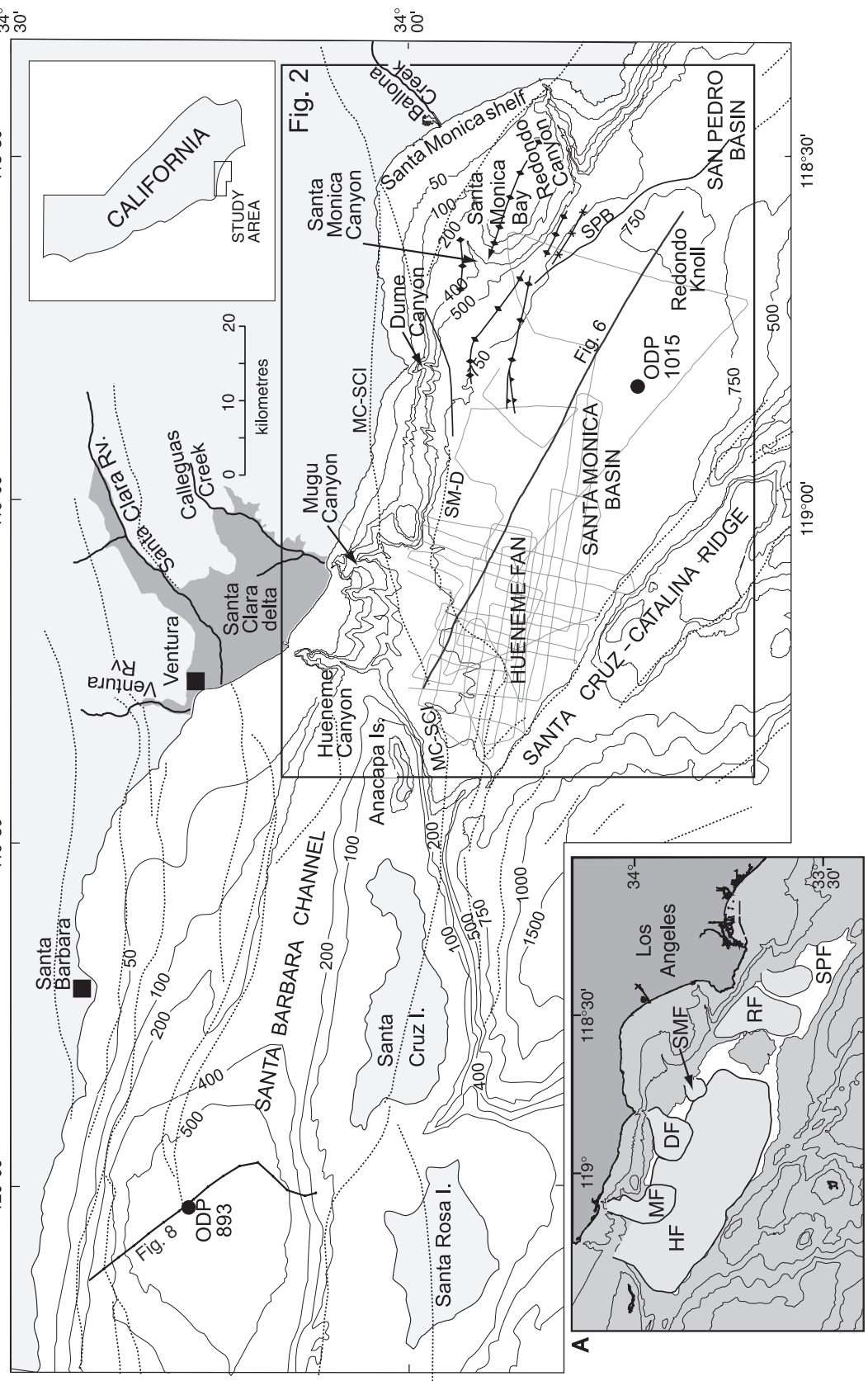

Fig. 1. Location map for the Santa Monica and Santa Barbara basins showing area of Fig. 2, location of ODP Sites 893 and 1015, and location of multichannel profiles in Figs 6 and 8. The names of the fault zones, shown with dotted lines, are informal because no uniform terminology has yet emerged from previous work; MC-SCI, Malibu Coast–Santa Cruz Island fault zone; SM-D, Santa Monica–Dume fault zone; SPB, San Pedro Basin fault zone. Schematic map at lower left shows the location of turbidite fans referred to in text: HF, Hueneme Fan; MF, Mugu Fan; DF, Dume Fan; SMB, Santa Monica Fan; RF, Redondo Fan; SPF, San Pedro Fan.

rivers with a high propensity for hyperpycnal flow (Mulder & Syvitski, 1995; Warrick & Milliman, 2003). The continental shelf is narrow and intersected by submarine canyons, so storm-generated turbidity currents are likely (Fukushima *et al.*, 1985). The region is seismically active, leading to slump-generated turbidity currents (Gorsline, 1996). Reliable age control on the pre-Holocene section has previously been lacking, so that the well-known post-glacial evolution of the basin has not been placed in a longer geological context. Two ODP wells in the northern California Continental Borderland now provide an opportunity to determine the chronology of the upper part of the seismic stratigraphy. New radiocarbon dates from ODP 1015 in the Santa Monica Basin (Normark & McGann, 2004) and published results from ODP 893 in the Santa Barbara Basin (Kennett & Venz, 1995) are used in this study to provide age control on the seismic stratigraphy.

The purpose of this paper is to use the new chronologic data and seismic-reflection profiles to evaluate how turbidite depositional processes have changed with changing sea level and tectonics. This involves interpretation of how sediment input points and the initiation processes of turbidity currents have changed through time, by comparison of the Hueneme Fan, fed directly by the Santa Clara Delta, with the smaller Mugu, Santa Monica and Dume fans in which longshore drift of sediment is important. Each of these fans, because of the particular morphology of its feeder canyon system, has responded in different ways to Late Quaternary sea-level change. The Hueneme Fan is discussed in less detail in this study than the other fans because its facies architecture has already been described elsewhere (Normark *et al.*, 1998; Piper *et al.*, 1999).

METHODS

This study combines new seismic-reflection studies by the US Geological Survey (USGS) to assess earthquake hazards with previous studies of turbidite sedimentation by the Geological Survey of Canada (Table 1). More than 3500 line-km of seismic-reflection profiles collected since 1990 have been interpreted; these data include single-channel and multichannel profiles and 1600 km of high-resolution deep-tow boomer seismic-reflection data, which were collected simultaneously with the deeper penetration reflection data. These new data provide the first direct seismic-reflection tie to ODP 1015. High-resolution seismic-reflection data were obtained using a Huntec DTS boomer system (Huntec Ltd., Toronto, Canada), towed about 100 m below the sea surface with heave and depth compensation. Acoustic signals were received on a 15 ft long, single-channel, 10-element oil-filled streamer (Benthos MESH 15/10P; Benthos Inc., North Falmouth, MA, USA) towed behind the fish containing the boomer source. Signals were filtered at 500–10 kHz with spreading-loss gain recovery. The source was operated at 500 J out-

Table 1. Summary of seismic-reflection data used in this study.

Year/cruise*	Data type	Line-km	Comments
1984/F-1-84-SC	Single-channel	62	40 $in.^3$ air gun
1985/W-40-85-SC	Multichannel	1203	1400 $in.^3$ air-gun array‡
1990/L-4-90-SC	Multichannel	124	2424 $in.^3$ air-gun array‡
1992/P-1-92-SC	Deep-tow boomer	854	Run simultaneously with air gun
1992/P1-92-SC	Single-channel†	854	40 $in.^3$ sleeve gun
1997/S-1-97-SC	Multichannel	165	35 $in.^3$ generator injector (GI) gun‡
1998/A-1-98-SC	Deep-tow boomer	780	Run simultaneously with GI gun
1998/A-1-98-SC	Multichannel	482	35 $in.^3$ GI gun‡
1999/O-1-99-SC	Multichannel	83	35 $in.^3$ GI gun‡
2000/A-1-00-SC	Multichannel	88	35 in^3 GI gun‡
2000/A-1-00-SC	Single-channel sparker	204	1·5 kJ minisparker
2002/A-1-02-SC	Single-channel air gun	75	24 in^3 air gun

*The cruise operation is associated with an activity identity, e.g. F-1-84-SC, which can be used to obtain metadata for the cruise at http://walrus.wr.usgs.gov/infobank/ where F-1 is an abbreviation for ship name and cruise leg, 84 is the year, and SC is the area (southern California).

†The sleeve-gun data from the 1992 cruise were recorded on two different systems providing different resolution of turbidite facies (see text).

‡Multichannel acquisition: 250 m long, 24-channel streamer for 35 $in.^3$ GI gun; 2·6 km long, 48-channel streamer for 2424 $in.^3$ air gun array; 2·9 km long, 120-channel streamer for 1400 $in.^3$ air-gun array.

Table 2. Seismic-reflection markers and their interpretation.

Marker	Dume Fan markers	Depth at ODP 1015 (m)	C-14 age (ka)	Cal. Age (ka)	Relationship to sea level
O	zz	2	1·5	1·5	
N	yy	9·5	4	4·5	
M	xx	14	6	7	End of transgression
L	ww	19	8·5	9·5	
K	vv				
J		33	13	14·5	
H	uu				
F		66 or 76*	20	24·5	Just before LGM
D		99	32	37	Start of rapid fall
C				55–60	
B				70	Stage 4 lowstand
A				95	Lowstand
Teal				115	Lowstand
Blue				130	Top MIS 6 lowstand
Brown					Top MIS 7
Orange					Top MIS 8 lowstand
Green					~Top MIS 9 highstand*
Yellow					Hemipelagic or distal turbidite

*See text for explanation.

put. The signal contains a broad-frequency bandwidth (up to 6 kHz), which yields an optimal vertical resolution of *ca* 0·25 m. Signal levels are generally sufficient to yield acoustic imaging up to 100 m below the sea floor. The acoustic facies terminology of Piper *et al.* (1999) is used to interpret the boomer data. This study incorporates the seismic marker horizons of both the Normark *et al.* (1998) and Piper *et al.* (1999) studies, in addition to providing correlative Huntec-scale markers on Dume Fan and deeper basin-wide markers (Table 2). High-resolution (i.e. two second sub-bottom records) multichannel seismic data were collected using a 35 cu. in. (573 cm^3) double-chamber generator-injector (GI) air gun and a 24-channel streamer with 10 m long groups of three hydrophones each. These data were migrated at 85% of the stacking velocity with the application of a 500 ms automatic gain control (AGC). In addition, a few single-channel profiles were collected using a 1·5 kJ minisparker. The interpretation has been augmented by review of industry and USGS deep-penetration multichannel data collected with large air gun array sources and >2 km long streamers (see Table 1).

Eleven new radiocarbon determinations from ODP 1015 (see Normark & McGann, 2004) have been made on picked fresh-looking foraminifera, where possible *Uvigerina* spp., but otherwise on mixed benthic or planktonic species (Table 3).

Table 3. Radiocarbon ages (from Normark & McGann, 2004).

ODP Hole 1015B Core section, sample interval	Sample depth (mbsf)	Sample description	NOSAMS no.	Age (year)	Age error (year)	Age reservoir corrected (year)
02H, 02W, 55–57 cm	4·35	Mixed benthic foraminifera	OS-35811	3430	45	1680 ± 45
02H, 03W, 144–146 cm	6·74	*Uvigerina* sp.	OS-35835	3850	40	2100 ± 40
02H, 04W, 101–103 cm	7·81	*Uvigerina* sp.	OS-35836	4720	30	2970 ± 30
02H, 06W, 12–14 cm	9·92	*Uvigerina* sp.	OS-35837	5530	35	3780 ± 35
02H, 07W, 55–57 cm	~11·68	Mixed benthic foraminifera	OS-39187	6940	70	5190 ± 70
03H, 02W, 119–121 cm	14·50	Mixed benthic foraminifera	OS-39188	8390	45	6640 ± 45
03H, 04W, 55–57 cm	16·85	*N. pachyderma*	OS-35838	9130	50	8330 ± 50
06H, 03W, 112–114 cm	44·36	*Uvigerina* sp.	OS-35839	15 950	60	14 200 ± 60
08H, 03W, 105–107 cm	63·35	*Uvigerina* sp.	OS-35840	21 300	95	19 550 ± 95
11H, 01W, 14–16 cm	87·95	Mixed benthic foraminifera	OS-39189	29 700	150	27 950 ± 150
12H, CCW, 28–30 cm	97·59	Mixed benthic foraminifera	OS-39190	33 500	220	31 750 ± 220

Analyses were made at the NOSAMS laboratory at Woods Hole. Marine reservoir corrections have been applied as follows: 800 years for planktonic foraminifera < 12 ka; 1100 years for planktonic foraminifera > 12 ka; and 1750 years for benthic foraminifera, following Toggweiler *et al.* (1989), Southon *et al.* (1990), Kienast & McKay (2001), and Kovanen & Easterbrook (2002). Dates are reported without calibration, but where correlation was made with a calendar time scale, the INTCAL98 procedure of Stuiver *et al.* (1998) was used for calibration, with the estimates of Bard *et al.* (2004) for the oldest ages.

GEOLOGICAL SETTING

The Santa Monica Basin, west of Los Angeles, is a north-west trending, 900 m deep ponded basin bounded on two sides by strike–slip faults and to the north by the narrow continental shelf of the Malibu coast. To the south-east, Redondo Knoll, a 400 m high asymmetric basement block, forms a sill between the Santa Monica and San Pedro basins (Figs 1 and 2), which are two of a series of basins bounded by oblique-slip faults in a generally transpressive tectonic regime (Vedder, 1987; Crouch & Suppe, 1993; Klitgord & Brocher, 1996). A transition from strike–slip faulting to reverse or thrust faulting occurs within Santa Monica Basin going from south-east to north-west (Fisher *et al.*, 2003), resulting in a complex history of displacement for many of the known faults. Pre-Quaternary strata along the margins of the basin show progressively increasing deformation with sub-bottom depth and the uplifted equivalents of these strata are known from outcrops on land and from wells in the Los Angeles basin (Wright, 1991; Normark & Piper, 1998; Fisher *et al.*, 2003). The east–west trending Malibu Coastal–Santa Cruz Island fault zone (MC-SCI) bounds the northern margin of the Santa Monica Basin. This complex fault zone has multiple names as a result of its complex segmentation, and the interpretation of Sorlien *et al.* (2003) is followed here. Along the base of the northern margin of the basin, the Santa Monica–Dume fault zone is another complexly segmented structure (Fig. 1). A series of north-

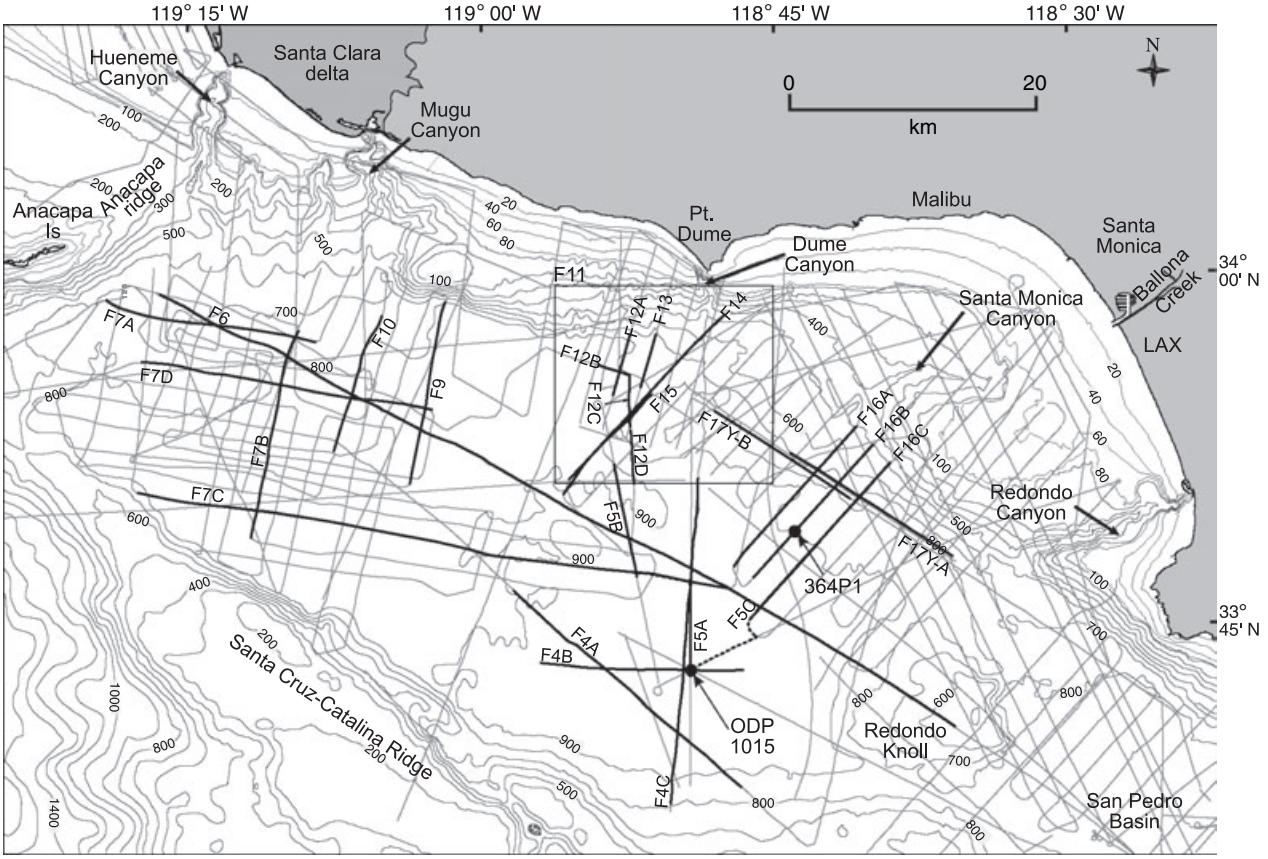

Fig. 2. Map of the Santa Monica Basin showing tracklines for seismic-reflection profiles use for study (light grey lines) and locations of profiles illustrated in subsequent figures (heavy, dark lines). Area of Fig. 11 shown. Bathymetric contours from NOAA (1998).

west to south-east trending dominantly strike–slip faults are active in the southern part of the basin and on its margins, including the San Pedro Basin fault zone (Fig. 1). Broderick *et al.* (2003) related deformation along the north-eastern margin of the basin to deformation associated with a buried thrust, which has formed an anticlinorium that underlies the shallow shelf area between the Santa Monica and Redondo Canyons (Fig. 2). Bohannon *et al.* (2004) correlated strata more than 200 msec. sub-bottom beneath the Santa Monica Basin with the Pliocene to late(?) Pleistocene Pico Formation exposed on land.

The regional morphology of Santa Monica Basin is known from conventional bathymetric charting, GLORIA long-range sidescan surveys (Edwards *et al.*, 1996), and multibeam bathymetry along the north-eastern margin adjacent to Santa Monica Bay (Gardner & Dartnell, 2002). Off the Santa Clara and Ventura rivers in the north, the shelf break marks the limit of late Pleistocene delta progradation (Nardin *et al.*, 1981; Dahlen *et al.*, 1990). Several submarine canyons incise the upper continental slope; and Hueneme, Mugu and Dume canyons eroded headward in the Holocene and intersect sediment moving south-eastward in the prevailing littoral drift system (Nardin *et al.*, 1981). The Hueneme Fan is the principal sediment accumulation in the Santa Monica Basin and has been supplied principally by the Santa Clara and Ventura rivers. The Hueneme Canyon leads to a 5 km wide fan valley with highly asymmetric levees (fig. 3 in Normark *et al.*, 1998). Since the early Holocene, an inner thalweg and small, sandy inner levees were formed within the fan valley, reflecting a diminution in sediment supply and the size of turbidity currents (Piper *et al.*, 1999). The fan valley diminishes in relief basinward. Near the 800 m isobath, it passes into a zone of mid-fan lobes, characterized by downfan-convex isobaths and broad shallow valleys < 5 m deep. The lower fan, which lacks recognizable lobes and has only rare shallow valleys, passes basinward into a flat-ponded basin plain. Sediment delivery processes during the late Holocene include earthquake-triggered slumping of pro-delta sediment and flood discharges of the Santa Clara River (Gorsline, 1996). In addition, Normark *et al.* (1998) inferred that some flows were generated by storm surges in the head of Hueneme Canyon, similar to the process described by Fukushima *et al.* (1985) in Scripps Canyon farther south. Piper *et al.* (1999) inferred that at times of stable lowered sea level, turbidity currents were produced principally from hyperpycnal flow during flood stages of the 'dirty' Santa Clara River (cf. Mulder & Syvitski, 1995).

Smaller sediment input points to the Santa Monica Basin are located at Dume Canyon and Santa Monica Canyon (Fig. 2). Dume Canyon is localized by Point Dume, which blocks the littoral drift system, and leads to a small submarine fan – the Dume Fan (Normark *et al.*, 1998). Santa Monica Canyon is at present inactive, but the new data (see below) show that it supplied sediment to Santa Monica Basin in the past. Santa Monica Canyon wraps around the northern end of a large anticlinorium that forms a wide shelf in the southern half of Santa Monica Bay. In the middle Pleistocene, the Silverado delta was built by an ancestral Los Angeles River now represented by the Ballona Creek. Redondo Canyon, at the south-eastern end of the littoral drift system in Santa Monica Bay, supplies sediment to the San Pedro Basin (Fig. 2).

In previous studies of the Hueneme Fan and Santa Monica Basin, Normark *et al.* (1998) and Piper *et al.* (1999) defined a series of seismic-reflection markers, A to O, that can be recognized on both air gun and Huntec boomer profiles (Table 2). This nomenclature is adopted in the present study. Marker horizons below A have been given colour designations (e.g. blue).

SEDIMENTOLOGY AND RADIOCARBON STRATIGRAPHY OF ODP 1015

The two holes at ODP Site 1015 (Shipboard Scientific Party, 1997) are used to determine the sedimentary character and age of sediment in the upper 150 m of the basin fill. The unpublished

Fig. 3. Graphical sedimentary log for ODP Site 1015 constructed from the visual core descriptions (VCDs) obtained from the Ocean Drilling Program archive at Texas A & M University. The log combines VCDs from Holes 1015A and B; vertical scale (mcd = metres core depth) reflects the combined logs. Radiocarbon dates are shown in bold numbers to the left of the logs and the bold letters refer to the basin-wide sequence of key reflectors (see text). The upper 20 m of the log is expanded (to the right) to better illustrate the relation between the radiocarbon dates and the late Holocene interval of key reflector stratigraphy. The graph at right shows the sediment accumulation rate (in mm yr^{-1}). The graph at lower right shows the number of turbidity-current events (per kyr^{-1}). The location of Site 1015 is shown in Figs 1 and 2.

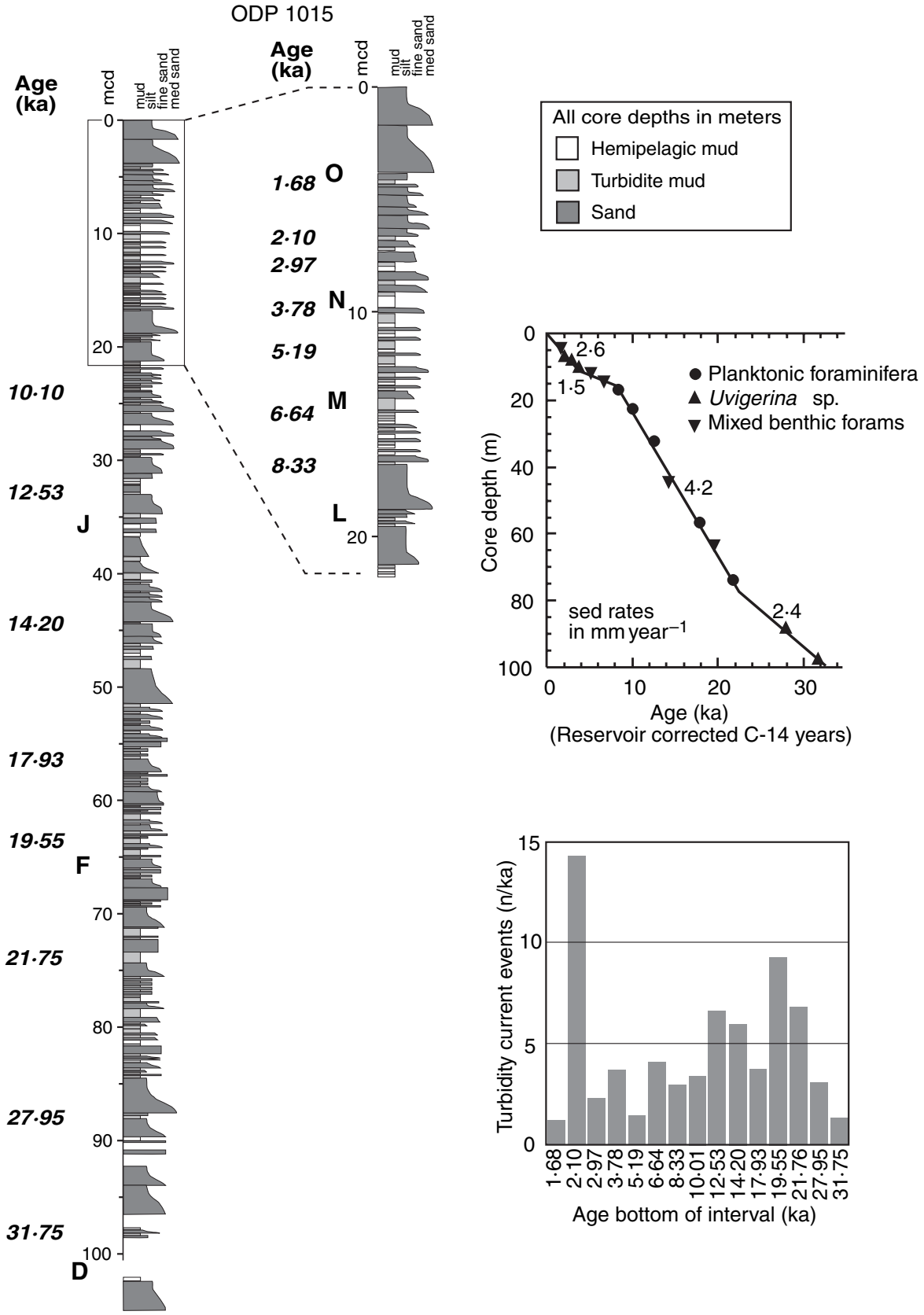

visual core descriptions from the two holes, available from ODP, were used to construct a composite stratigraphic column (Fig. 3) based on Hole 1015B, with missing or deformed intervals correlated from Hole 1015A. Hole 1015B was drilled to 98·7 metres below sea floor (mbsf) using the advanced piston corer, but the deeper part of Hole 1015A to 149·5 mbsf required rotary drilling, so that core recovery was lower, sands were badly disturbed, and recognizable hemipelagic intervals were not logged. Offset holes were drilled at Site 1015 to ensure core recovery of all stratigraphic intervals for palaeoclimate studies.

Some intervals, such as 0–4 and 18–21 mbsf, recovered thick-bedded graded sand beds. In other intervals, such as 8–17 mbsf, sand beds are thin but overlain by thick turbidite mud capped by lighter coloured, bioturbated hemipelagic mud. In other intervals, such as 52–67 mbsf, sand bed thickness is more variable, most are capped by turbidite mud, and hemipelagic mud beds are rare. The clear development of graded sand to mud beds allowed the number of sand-transporting turbidity current events to be counted over most core intervals (inset, Fig. 3). The location of the well on the flat basin floor, the lack of evidence for sand-on-sand amalgamation and the presence of interbedded hemipelagic sediment suggest that there was not significant erosion of previously deposited turbidites.

Radiocarbon accelerator mass spectrometry (AMS) age determinations (Table 3) were made on foraminifera from hemipelagic intervals in ODP 1015B in order to develop an age model for the entire basin through seismic-reflection correlation. Ages are reported in radiocarbon years (i.e. are not calibrated) and have been corrected for the marine reservoir effect. An age of 31·75 ka was obtained at 97·6 mbsf at the base of Hole 1015B. The foraminiferal assemblage from ODP Site 1015 (Shipboard Scientific Party, 1997, p. 228) shows the following correlations with the well-dated biostratigraphy at ODP Site 893 in the Santa Barbara Basin (Fig. 1; Kennett & Venz, 1995): At 64–74 mbsf, the peak in *Neogloboquadrina pachyderma* (dextral) indicates an age of 18 ka and at 140–150 mbsf, the common *Globigerina bulloides*, common and then absent *N. pachyderma* (sinistral) and the few *N. pachyderma* (dextral) indicate an age of 30–35 ka (Normark & Piper, 1998).

Sedimentation rates on the ponded basin floor averaged 2·6 mm yr^{-1} in the late Holocene, with a turbidite event every 290 years on average (Fig. 3). During and following the early to middle Holocene transgression, after flooding of the Pleistocene Santa Clara delta at about 9 ka, rates were lower at 1·5 mm yr^{-1} with a turbidite event every 350 years. Throughout the MIS 2 lowstand, sedimentation rates consistently averaged 4·2 mm yr^{-1} with a turbidite every 175 years. Sedimentation rates diminished to a less well-constrained 2·4 mm yr^{-1} during the falling sea level of the MIS 3 to 2 transition, with a turbidite every 415 years (Fig. 3).

Seismic-reflection ties from ODP Site 1015 to other parts of the Santa Monica Basin are illustrated in Fig. 4 for deeper reflectors using air-gun profiles and in Fig. 5 for shallower reflectors using Huntec boomer profiles. The flat-lying character of sediment fill in the basin plain is evident from examples in Fig. 4. There is ample evidence for gas accumulation within these distal turbidite deposits, including bright (high-amplitude) reflections, velocity–amplitude anomalies (vamps), and the presence of a mud volcano near the mouth of Redondo Canyon where methane hydrate has been recovered (Normark *et al.*, 2003). The high sand content of these basin plain deposits (see bulk density profile, Fig. 5) provides the permeability needed for gas to migrate across the basin. The uppermost key reflectors at Site 1015 can be correlated to piston core site 364P1 on the lower slope of the basin (Figs 2 and 5C). Radiocarbon dating of samples from this core confirm that changes in sedimentation rate observed at Site 1015 are mimicked on the lower slope, thus indicating that many of the turbidity-current flows reaching the basin floor were at least 35 m thick (Normark & McGann, 2004).

FANS ON THE NORTH-EASTERN MARGIN OF THE SANTA MONICA BASIN

The Hueneme Fan, located seaward of the Santa Clara–Ventura delta, has already been discussed

Fig. 4. Seismic-reflection profiles showing basin-floor stratigraphy of the Santa Monica Basin at ODP Site 1015. Profile identities shown in lower right corners for each line. (A) 40 cu. in. sleeve gun source; (B) multichannel air-gun record adapted from Lyle *et al.*, 1995; (C) single-channel sparker source. Key basin-wide stratigraphic reflectors C, D, and J in these profiles can be traced throughout much of the basin; refer to Fig. 5 for reflectors between J and the sea floor and see text for explanation. Profile locations shown in Fig. 2. All profiles show evidence for gas accumulation in the sediment below about 0·25 sec two-way travel time as high-amplitude (bright) reflections.

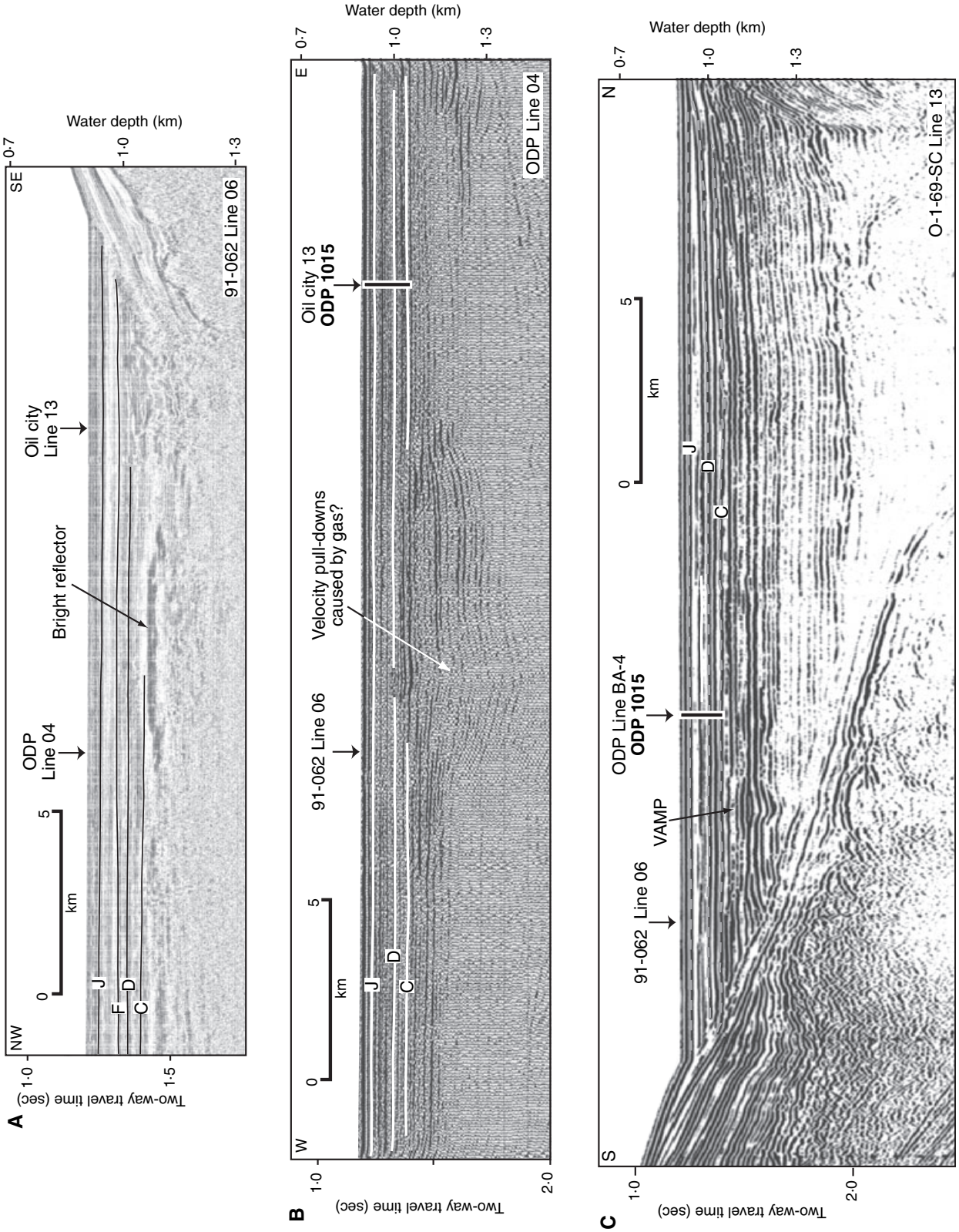

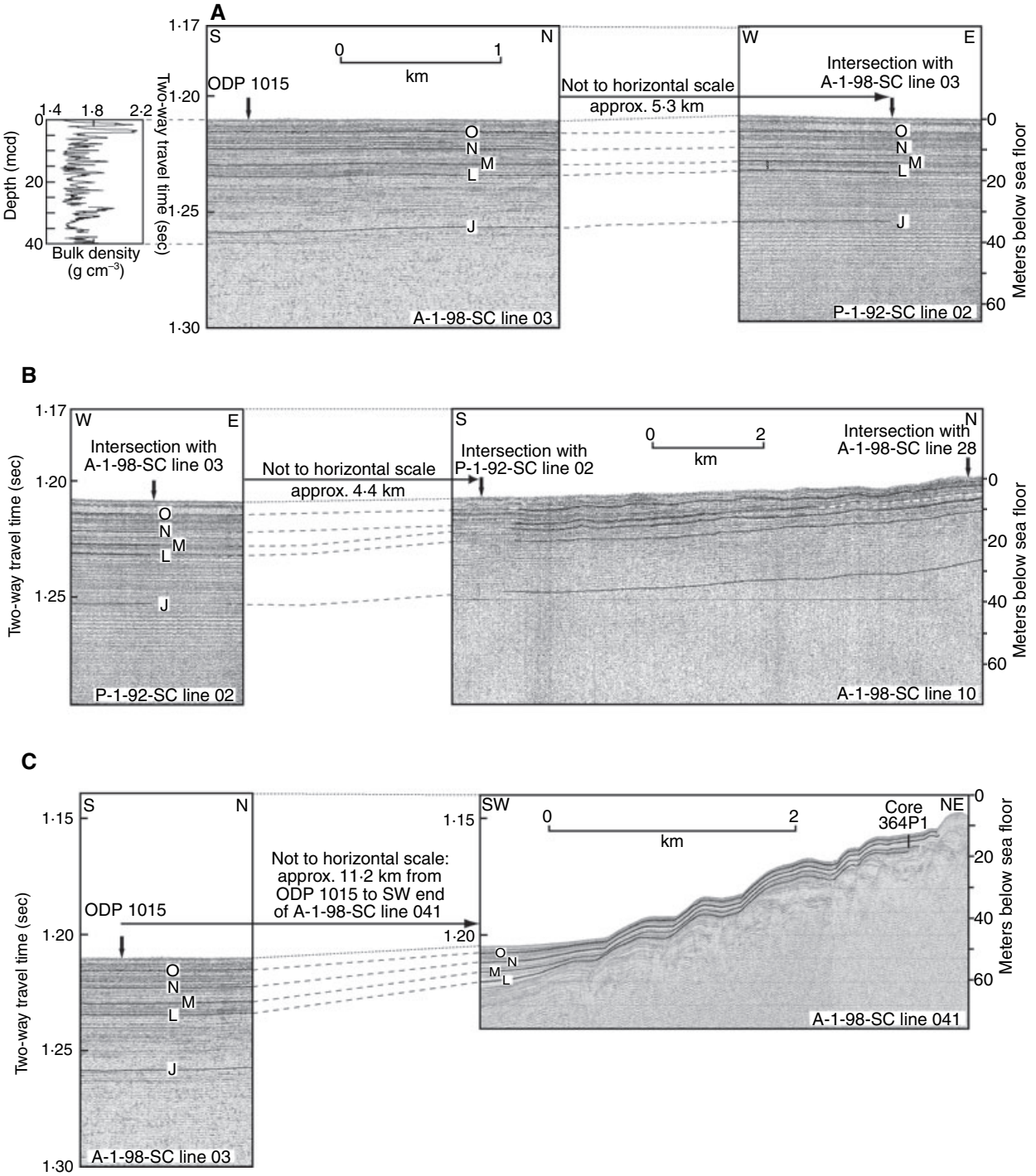

Fig. 5. High-resolution deep-tow boomer profiles keyed to ODP Site 1015 and used to extend the key seismic markers O to J throughout the basin. See Fig. 2 for location. Line 2 from Geological Survey of Canada (GSC) cruise 91-062; other lines from US Geological Survey cruise A-1-98 (Table 1). (A) Tie to Hueneme Fan through P-1-92 line 02; (B) tie to Dume Fan; (C) tie to core 364P1 (see text).

at length in previous papers (Normark *et al.*, 1998; Piper *et al.*, 1999; Piper & Normark, 2001) and its evolution back to reflector A is well established. A deep multichannel seismic-reflection line (L490-125) is interpreted, in this study, to provide new insight into earlier evolution of Hueneme Fan (Fig. 6). New stratigraphic information is also presented for the Mugu fan, a smaller sediment body fed by Mugu Canyon, located at the eastern edge of the Santa Clara–

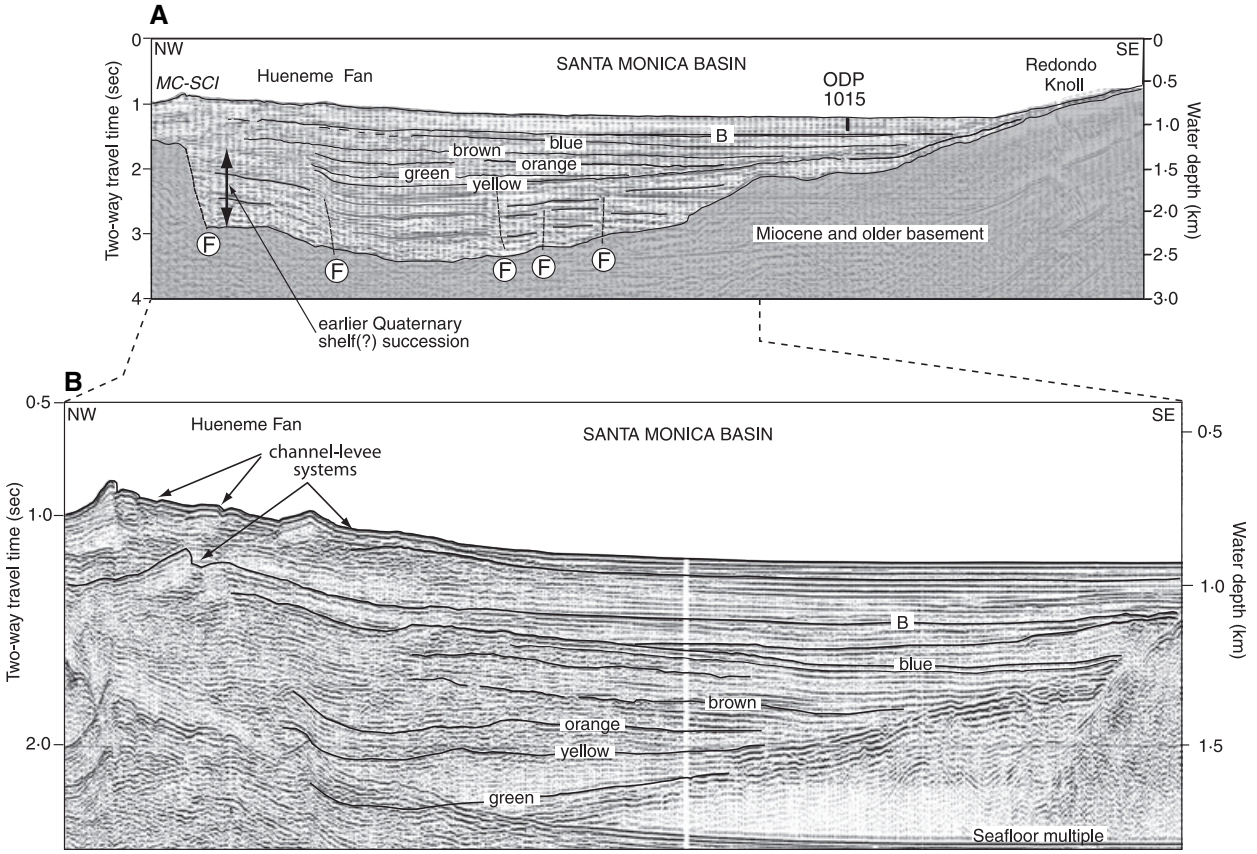

Fig. 6. (A) Schematic interpretation of multichannel profile L-4-90 Line 125 extending from the upper Hueneme Fan to Redondo Knoll. MC-SCI: Malibu Coast–Santa Cruz Island fault zone. (B) Reflection profile from the same line over the main part of Hueneme Fan. See text for explanation of letter and colour designations for interpretation in (A). Circled F indicates fault. See Fig. 1 for location.

Ventura delta (Fig. 1 inset). At low stands of sea level, the entire Hueneme–Mugu fan system prograded as a result of multiple sediment input points from the Santa Clara–Ventura delta, but at other times the Hueneme and Mugu canyons acted independently and built discrete fans. A new stratigraphic interpretation of the Dume and Santa Monica fans farther east is also described.

Deep structure of Santa Monica and Santa Barbara basins

Representative multichannel seismic profiles from both the Santa Monica and Santa Barbara basins are interpreted in order to understand the middle to late Quaternary history of the Hueneme Fan and the Santa Monica Basin. Multichannel seismic line L490-125 (Fig. 6) extends from the upper part of Hueneme Fan to the south-west end of Santa Monica Basin (Fig. 1) and is correlated with ODP Site 1015 through Oil City line 13 (Figs 2 and 4C). Basement rocks older than Middle Miocene underlie the north-west end of the profile and step up across a series of faults towards the Anacapa ridge. They also rise to near the sea floor on Redondo Knoll (Bohannon *et al.*, 2004, their fig. 21). Flat-lying reflections of the Santa Monica basin plain progressively onlap south-eastward – a reflection that lies a short distance above basement over Redondo Knoll (yellow reflector in Fig. 6A). These flat-lying reflections are characteristic of a turbidite basin-plain architecture and pass north-westward into a more mounded seismic facies characteristic of a mid-fan architecture. One development of the latter facies lies above the regional C reflection and corresponds to the Hueneme mid-fan imaged with air-gun profiles (Fig. 7). The C to B interval was deposited uniformly over the Hueneme Fan and the ponded basin floor, with some lenticularity and high-amplitude reflections on the basin floor seaward of Santa Monica Canyon (e.g. compare Fig. 7C and D). The B to blue interval is thicker on the basin floor and thins where it onlaps towards the basin margin (Fig. 6A). In the blue to brown interval, there is again a thick

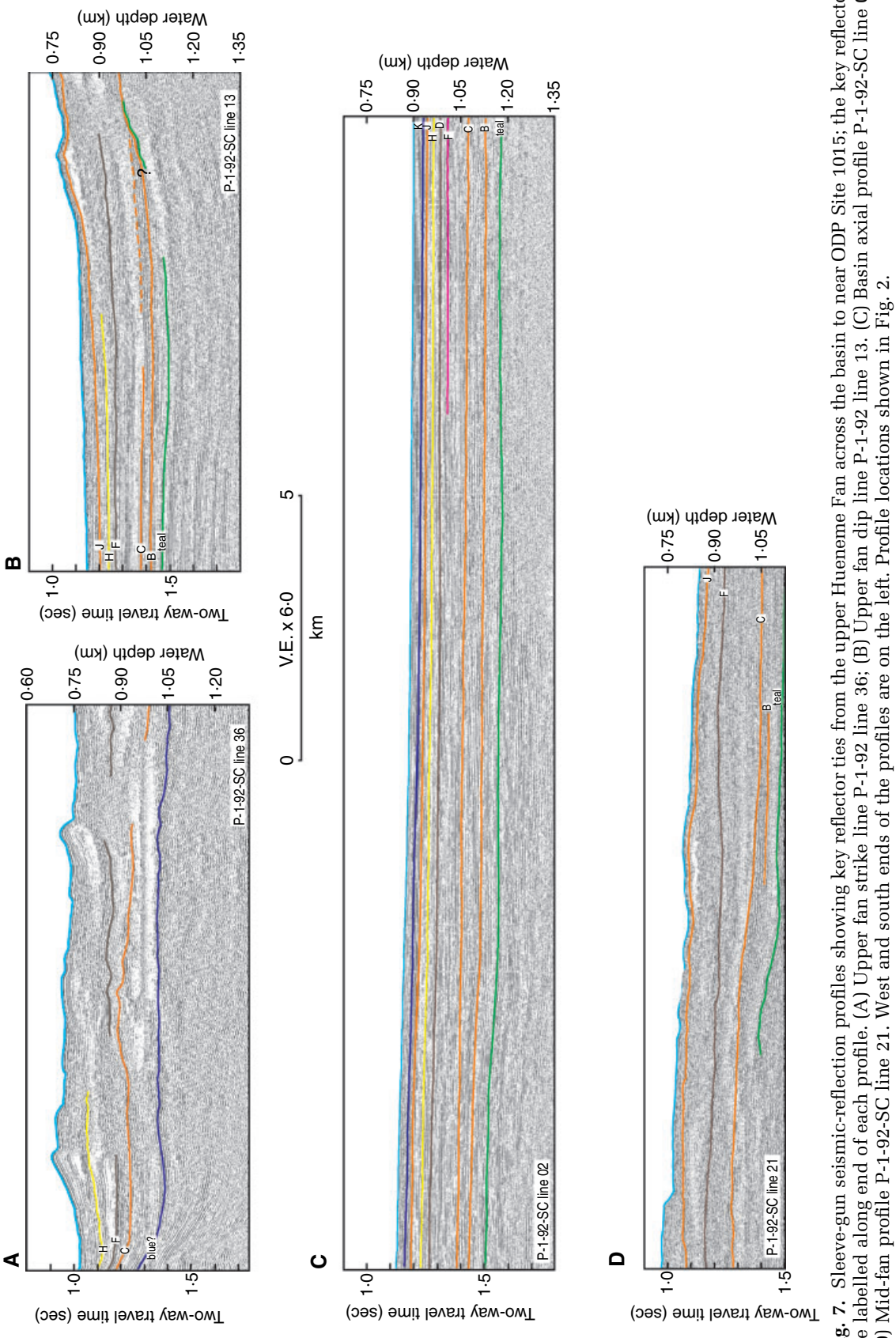

Fig. 7. Sleeve-gun seismic-reflection profiles showing key reflector ties from the upper Hueneme Fan across the basin to near ODP Site 1015; the key reflectors are labelled along end of each profile. (A) Upper fan strike line P-1-92 line 36; (B) Upper fan dip line P-1-92 line 13. (C) Basin axial profile P-1-92-SC line 02. (D) Mid-fan profile P-1-92-SC line 21. West and south ends of the profiles are on the left. Profile locations shown in Fig. 2.

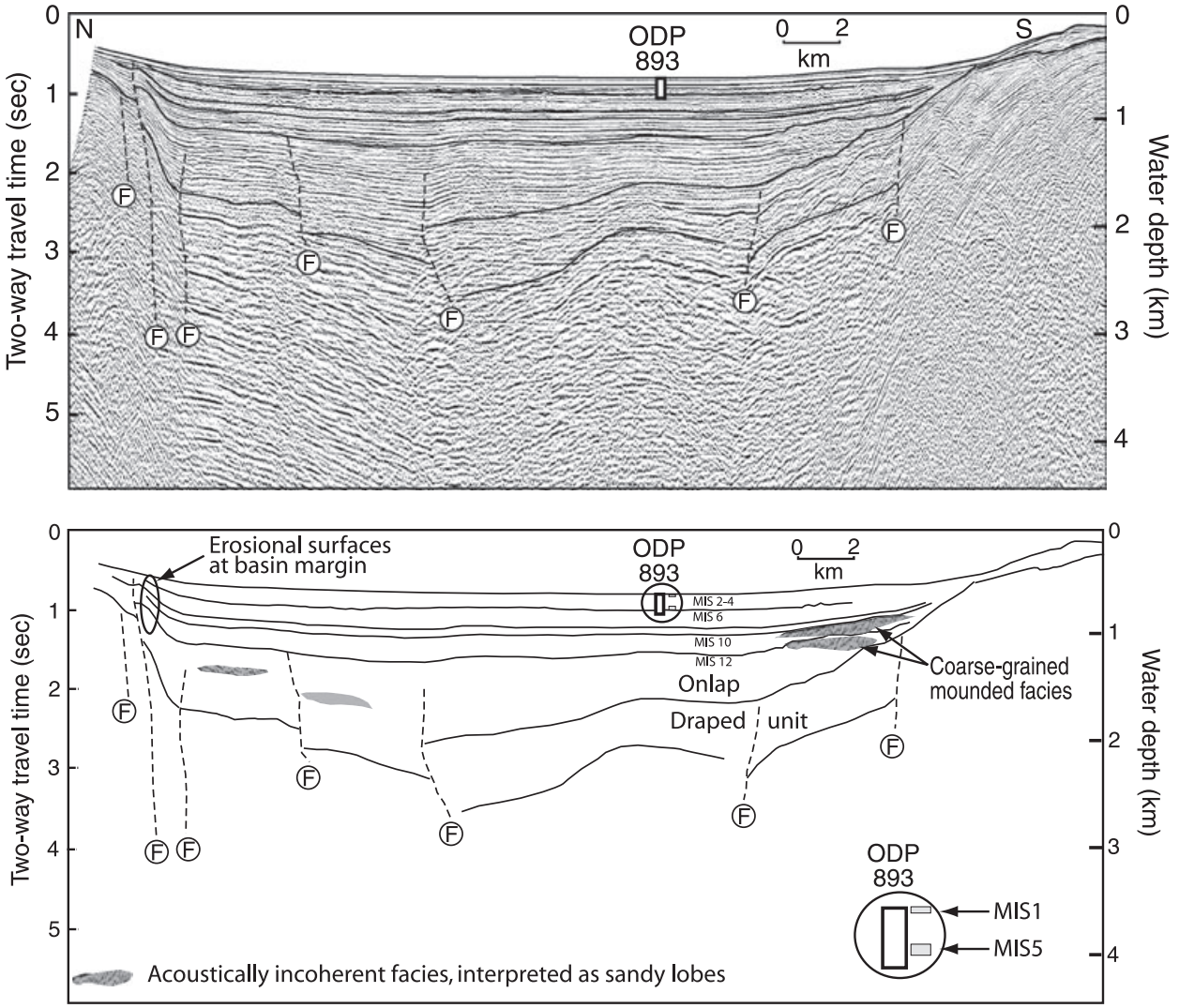

Fig. 8. (A) Multichannel reflection profile L-4-90 Line 107 across the Santa Barbara Basin and tie to ODP Site 893. (B) Schematic interpretation of Line 107. See text for explanation and Fig. 1 for location.

development of mounded facies beneath Hueneme mid-fan (Fig. 6A). The brown to orange interval is relatively uniform, with apparent basin-floor facies extending beneath the modern Hueneme Fan and onlapping the southern flank of Anacapa ridge. In the orange to green interval, mounded facies occupying the centre of Santa Monica Basin, south-east of Dume Canyon, passes into more regularly stratified facies both to the north-west and south-east (Fig. 6A and B). The underlying green to yellow interval is quite transparent.

The yellow reflection marks a change in sedimentation and perhaps in tectonism. The green, orange and brown reflectors onlap the yellow reflector on the flank of Redondo Knoll. In the central part of the basin, reflections below yellow are subparallel, continuous, and locally offset by faults (Fig. 6). They tend to drape irregularities on the basement surface. This reflection style and architecture is characteristic of predominant hemipelagic sedimentation, such as in the Santa Barbara Basin (Fig. 8). At the northern end of the basin, these reflectors rise against and locally onlap the fault-bound margin of a block of stratified sediment (Fig. 6A, left-hand side). In this block, the interval between yellow and the basement shows less continuous reflections, with a few prominent reflectors resembling transgressive erosion surfaces, and it is tentatively interpreted as an earlier Quaternary shelf succession.

The absence of fan and basin-floor turbidite facies in the Santa Monica Basin below the yellow reflection led to an examination of multichannel

seismic-reflection profiles from the Santa Barbara Basin, to evaluate whether the Santa Clara River contributed significant coarse-grained sediment to the Santa Barbara Basin in the past. Multichannel line L490-107 (Fig. 8) crosses the eastern side of the basin floor, passing through ODP Site 893. The basin fill consists of flat-lying reflections that onlap at the basin margin and at more than 1 s sub-bottom show fault offsets. At 2 sec sub-bottom in the centre of the basin, the basin fill onlaps a succession 0·7 sec thick that drapes over the basement and becomes shallower towards the southern margin of the basin. Above the prominent onlap surface, the southern part of the basin has uniform sedimentation. The only features that might represent a sandy submarine fan fed by the Santa Clara delta are intervals of more mounded deposition below 1 sec sub-bottom in the northern graben and indistinct lenses of less coherent reflections at 0·5 to 1·1 sec sub-bottom at the southern margin of the basin (grey tone in Fig. 8).

Mugu Fan

Bathymetry and morphology

Mugu Fan is a lobe of sediment on the north-eastern margin of Hueneme Fan that appears to have been derived from Mugu Canyon. This canyon is located at the eastern margin of the Santa Clara–Ventura delta (Fig. 1 inset). At sea-level highstands, its position is analogous to Dume and Redondo canyons, just west of a headland at the end of a littoral-drift cell. At lowstands, it would have received direct sediment supply from the Calleguas Creek drainage. This would also be the case at times when the Santa Clara and Ventura rivers flowed along the south-eastern margin of the delta plain, as a result of channel shifting resulting from autocyclic processes or tectonic tilting.

Seismic stratigraphy and facies distribution

Seismic-reflection profiles show a rather uniform sediment thickness across the Mugu Fan from reflection C to J (Fig. 9). Above J, there is a prominent mid-fan lobe that pinches out rapidly southwards against a much less-pronounced mid-fan lobe of the Hueneme Fan that was constructed between reflections D and J. This Mugu mid-fan lobe comprises incoherent acoustic facies immediately above J (sandy lobe deposits) passing up into well-stratified facies (upper-fan overbank facies, with local channels), using the interpretation of acoustic facies of Normark *et al.* (1998) and Piper *et al.* (1999) shown in Table 4. More stratified facies are also developed between reflections F and D and overlie a small incoherent mid-fan mound at a horizon near reflection D.

Below C, the sediment is deformed along an active reverse fault zone, which created a low ridge and then a small depression at the foot of the continental slope, within which mid-fan incoherent acoustic facies are well developed. South of this ridge, a mid-fan lobe with incoherent facies is developed approximately at reflection B and another is interpreted between reflections A and teal (Fig. 9).

In high-resolution Huntec boomer profiles (Fig. 10), only stratigraphic marker M and above are tied directly, but a muddy mass-transport deposit near the southern end of the line can be correlated with the deposit immediately overlying L higher on the delta, illustrated in fig. 9D of Piper *et al.* (1999). Below L, a 1·3 km wide sandy channel is flanked to the north by muddy levee deposits with interbedded sand (resembling fig. 7a of Piper *et al.*, 1999) and to the south by more irregular sandy wedges interbedded with well-stratified acoustic facies, resembling the east end of fig. 5a of Piper *et al.* (1999). The underlying sandy lobe deposits (Fig. 10, lower panel) are near the limit of penetration of the acoustic energy: the transition from these deposits to the channel–levee system corresponds approximately to K. Above N, subparallel moderate-amplitude reflections are present (acoustic facies II of Piper *et al.*, 1999; Table 4), with more irregular stratification of acoustic facies V in places between N and M.

Dume Fan

Bathymetry and morphology

Dume Fan is a 5 km wide fan with a classic fan-like pattern shown in bathymetry. It is fed by a canyon–fan valley system that heads within a few hundred metres of the coastline just on the west side of Point Dume, at the eastern end of a coastal longshore drift cell (Nardin *et al.*, 1981). Multibeam bathymetry (Fig. 11A) shows an amphitheatre-like canyon head with several feeder gullies. This feature narrows at about 500 mbsl to a gently sinuous fan valley that passes through a sharp meander bend at 600 mbsl. The fan valley then trends WSW to the basin floor east of Mugu Fan.

Shallow seismic stratigraphy

The shallow seismic stratigraphy is interpreted from Huntec boomer profiles. A local strati-

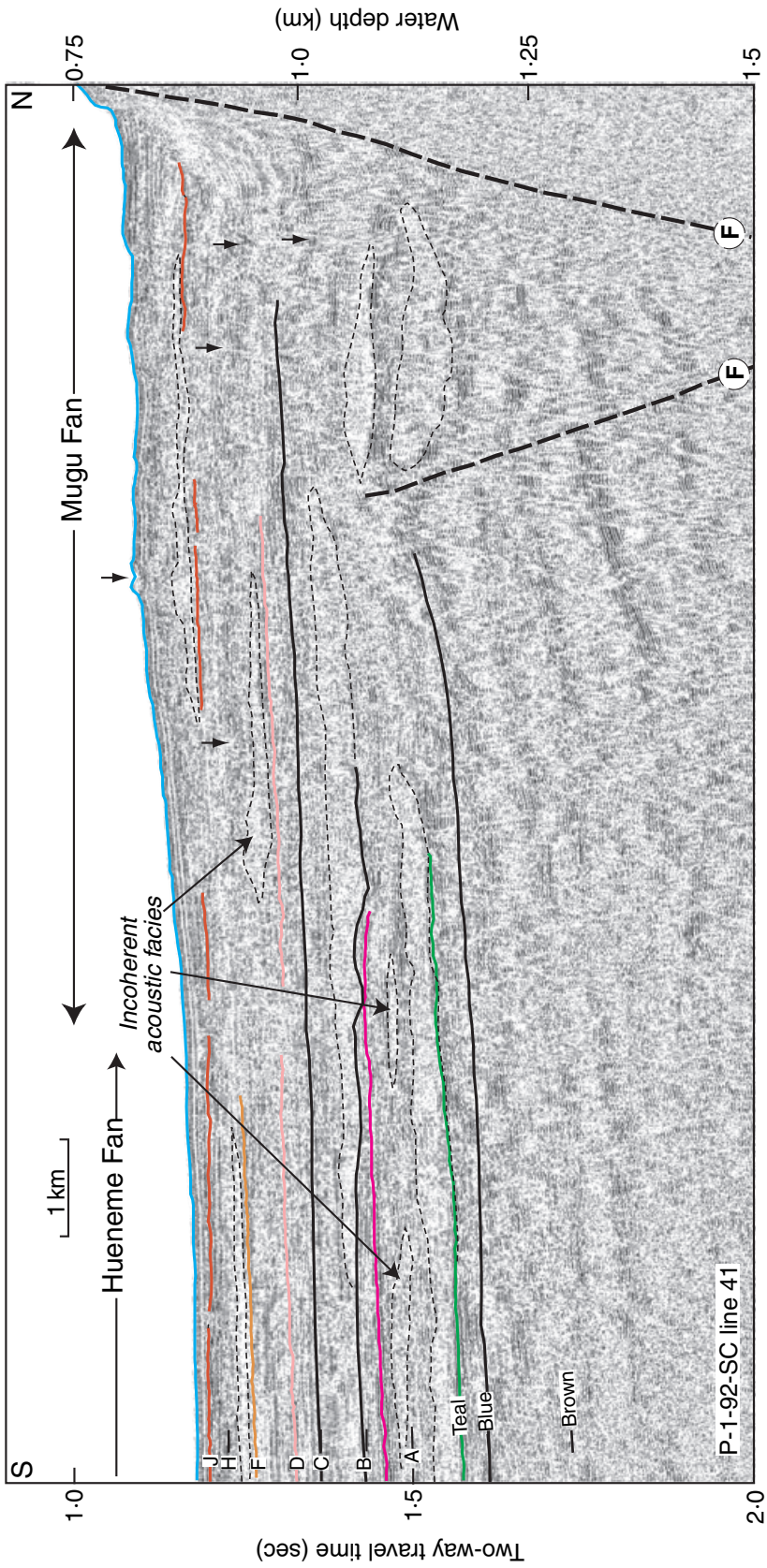

Fig. 9. Sleeve-gun seismic-reflection profile P-1-92 line 41 showing key reflector ties to the Mugu Fan. Small vertical arrows indicate small channel–levee systems. Dashed lines outline incoherent acoustic facies also identified from Huntec profiles (facies VII) in the shallow part of the section. Circled F indicates fault. Profile location shown in Fig. 2.

Facies	Brief description of reflections	Interpretation
I	Parallel, low amplitude	Mud, rare silt beds
II	Parallel, moderate amplitude	Mud, some silt and sand beds
III	Parallel, high amplitude	Mud, common silt and sand beds
IV	Discontinuous subparallel with incoherent intervals	Mud, some thick sand beds
V	Discontinuous, irregular	Mud, discontinuous sand beds
VI	Incoherent, high backscatter, some high-amplitude continuous	Thick sand beds, some mud beds
VII	Incoherent, high backscatter	Thick sand beds
VIII	Incoherent, low backscatter	Muddy mass-transport deposit

Table 4. Summary of acoustic facies in boomer profiles (from Piper *et al.*, 1999).

graphic scheme is defined that is then tentatively correlated with the reference section at ODP site 1015 (Fig. 5). Precise correlation of the interval from K to L is not possible because of onlap along the southern margin of Dume Fan. Much of the fan is underlain by mud with low amplitude reflections (acoustic facies I), corresponding to mud with thin silt laminae in cores (core SMB1) (Fig. 12C). At the morphological contact with the flat basin floor, this facies is onlapped by parallel moderate- to high-amplitude reflections (acoustic facies II, III) corresponding to sand and interbedded mud in cores. Core SMB3 failed to penetrate past a surficial mud layer suggesting sand-rich sediment (SMB3 was located about 2 km west of the position shown in brackets in Fig. 12D). The fan valley floor returns incoherent, high backscatter reflections (acoustic facies VII). The upper fan valley cuts facies I and does not have morphologically well-defined levees. On the lower fan valley, there is a clear levee form, with incoherent high-backscatter units (acoustic facies VI) and high-amplitude parallel reflections (facies III) wedging out away from the channel (Fig. 12B). On the north side of the lower fan valley, part of the thick mud drape appears to have been eroded out, with a 5 ms section of facies II overlying the erosion surface (Fig. 12A).

The seabed to zz (∼O) interval consists of transparent acoustic facies I in most places, with a few higher amplitude and more irregular reflections within 500 m of the lower fan valley (Fig. 12B). The zz (∼O) to yy (∼N) interval is transparent acoustic facies I in most places, but within 1 km of the lower fan valley, it has irregular stratification, high-amplitude reflections, and a clear overall wedge-shaped geometry (Fig. 12B). At the erosional edge of the thick transparent section north of the lower fan valley (Fig. 12A), the yy (∼N) reflector marks the top of a prominent wedge (about 1 km long) of high-amplitude reflections, analogous to the wedges forming levees adjacent to the fan valley. Below yy (∼N) on the north-west levee of the lower fan valley, the section was poorly penetrated by the boomer, suggestive of sand. A more transparent inner levee is developed on the south-east side of channel (Fig. 12B), filling a wider older channel beneath the present channel, the top of which corresponds to a horizon at −15 ms on the basin floor. On the east side of fan, yy (∼N) is a higher amplitude reflection in the middle of a thick transparent section. Passing off the fan onto the basin floor, the section above yy (∼N) doubles in thickness and the yy (∼N) to zz (∼O) interval has some inferred sand lenses at the break in slope (Fig. 12D).

The xx (∼M) reflection is a major onlap surface at the basin margin (Fig. 12D). On the east side of the fan, it marks the top of a thin, more reflective package with erosion and/or sediment-wave growth near the levee crest. It is the top of a package of reflective stratified sediment on the mid-fan. On the lower fan, it is simply a high-amplitude reflection within a transparent section. Beneath xx (∼M), the south-eastern levee crest of the older, wider valley is approximately marked by the ww (∼L) reflector (Fig. 12B and C). On the fan south-east of the fan valley, xx (∼M) to ww (∼L) is stratified levee sediment (facies II) near the old levee crest (Fig. 12C), stratified high-amplitude reflections on the mid-levee (facies IV, probably spillover sand alternating with mud), and transparent facies II on the lower fan. Below ww (∼L), stratified levee facies II persists near the levee crest, but an incoherent unit 10–25 ms thick with a reflective surface of bedforms underlies the lower fan (Fig. 12D) and appears to have prograded across the vv (K) reflector. This feature can be mapped across several seismic-

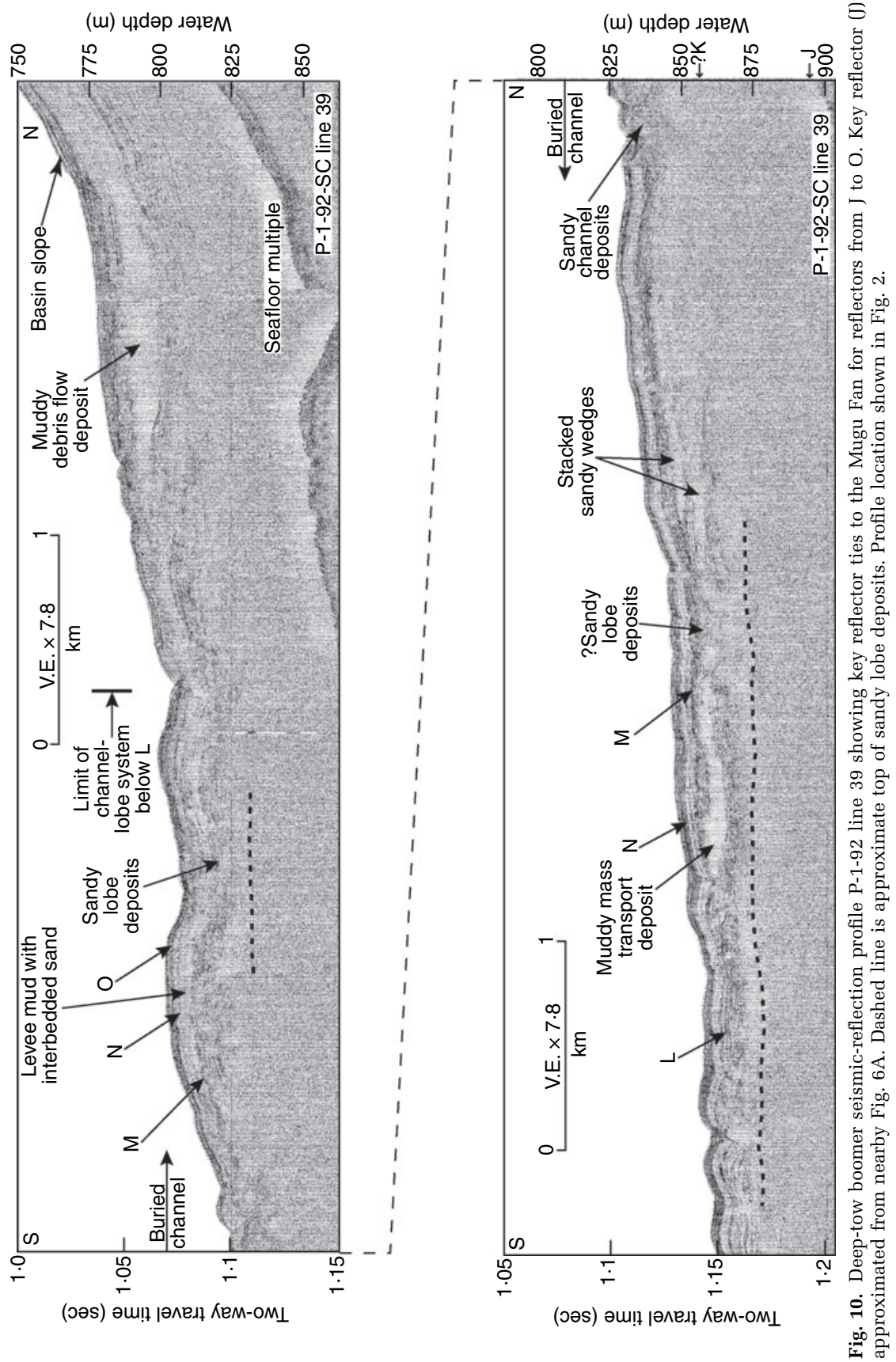

Fig. 10. Deep-tow boomer seismic-reflection profile P-1-92 line 39 showing key reflector ties to the Mugu Fan for reflectors from J to O. Key reflector (J) is approximated from nearby Fig. 6A. Dashed line is approximate top of sandy lobe deposits. Profile location shown in Fig. 2.

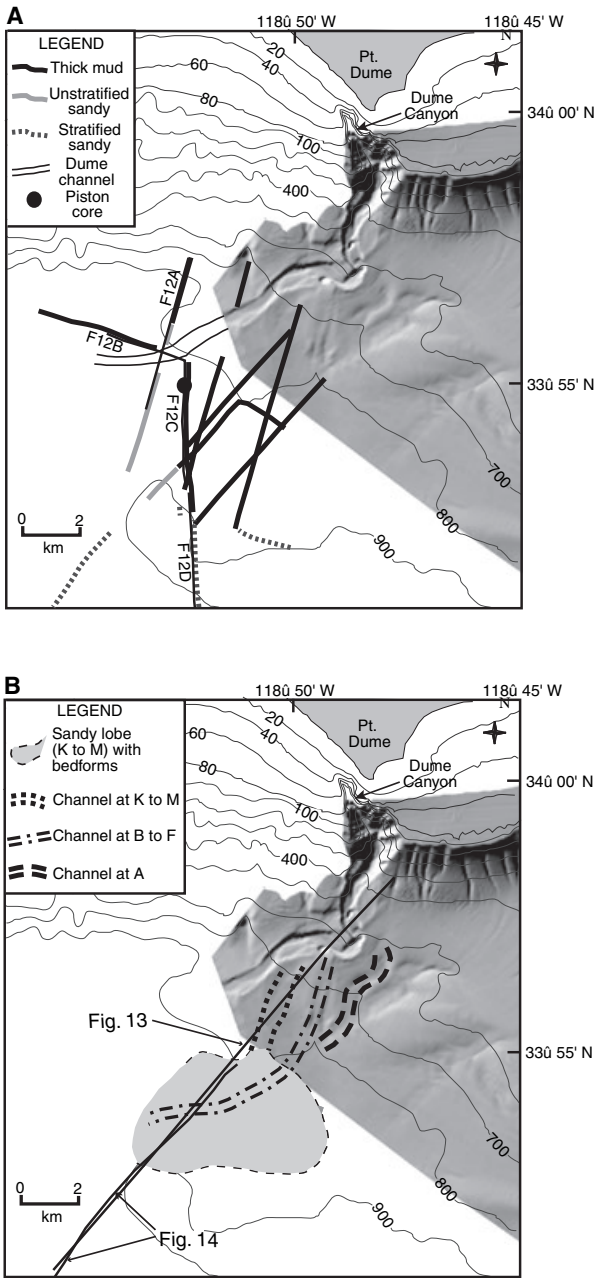

Fig. 11. (A) Multibeam image of the Dume Fan showing distribution of surface facies based on interpretation of deep-tow boomer profiles. (B) Multibeam image of the Dume Fan showing channel and lobe features in the K (vv) to M (xx) interval based on interpretation of deep-tow boomer profiles. Map location shown in Fig. 2.

reflection lines and appears to represent a termination lobe from a channel that turned southward to the west of the main meander on Dume fan valley (Fig. 11B). Beneath vv (K), well stratified sediment is visible in both Huntec boomer (Fig. 12D) and minisparker profiles (Fig. 13), except within 1 km of the present lower fan valley where there is a thick incoherent (presumably sand) section resting on a 1·5 km wide erosional surface marking a broad fan valley at uu (H) (Fig. 13).

Deep seismic stratigraphy

Seismic marker horizons are traced from the floor of Santa Monica Basin (Figs 4 and 6A) to Dume Fan via multichannel seismic line 29 (Fig. 14) and high-resolution air gun line PZ57 (Fig. 15). The shallowest reflections above C are almost horizontal on the basin floor (Fig. 14) and onlap the toe of Dume Fan (Fig. 15). Given the amount of tectonic uplift along the north-eastern margin of the Santa Monica Basin (Fisher *et al.*, 2003), it is likely that the deeper reflectors from C to orange, which dip south-westward, were originally horizontal basin floor deposits derived largely from Hueneme Fan and have subsequently been tilted. On line 54, which is the same line shown for Fig. 12B, deformation by the prominent reverse fault affects strata to above reflector B.

Below the blue reflector, Dume Fan appears sandy, but this character ends abruptly at the basin floor (Fig. 15), locally with wedges similar to the high-gradient lobes of Piper *et al.* (1999) [(w) in Fig. 15]. In the Blue to A interval, high-amplitude, irregular reflections are present on the lower fan (Fig. 15) that pass up-fan into an erosional surface over much of mid-fan (Fig. 14) including an incised channel system seen on line A100SC-322N (not illustrated; the profile is 4 km from and parallels the profile shown in Fig. 13), the infilled remnant of which is visible in multibeam imagery (Fig. 11B). This channel appears to have switched eastward at the prominent meander loop, at or just above horizon A. Below horizon B, a channel is visible just down-fan from the meander bend (Fig. 14). In the A to B interval, there are small channels with transparent fills with surface hyperbolic echoes (?debrisflow) and levee-like mounds on the lower fan (Fig. 15) and the main channel appears to have flowed to the south–south-east (Fig. 11B). Just above A, there is a high-gradient lobe, onlapping up-fan onto a low-relief levee (Fig. 15). From B to F, much of the lower fan has lenticular bodies, of uncertain origin, but likely a mix of low levees and lobes. On the upper fan, there is a rather thin overbank section (Fig. 14). Reflector F appears to be an erosional surface in many areas. The overbank section above F on the western part of the fan is particularly thin, as a result of incision and/or westward shifting of the main fan valley. Seismic

profile PZ54, illustrated by Normark *et al.* (1998), figs 6 and 11) shows onlap of basin floor sediment onto the western fan between horizons F and J, when the main channel discharged southward; then several channel-termination lobes developed above J as the main channel shifted to the north-west (Fig. 11B).

Santa Monica Fan

Bathymetry and morphology

The Santa Monica Fan is a buried feature seaward of Santa Monica Canyon (Figs 16 and 17). The canyon incises the outer part of the 10–15 km wide Santa Monica shelf and was probably fed by Ballona Creek at lowstands of sea level. Santa Monica Canyon leads to an apparently inactive shallow fan valley (Fig. 17B) and a low bathymetric feature on the south-eastern margin of the Santa Monica Basin (Fig. 16C). Much of the canyon is influenced by growth faulting where it crosses the plunging anticline that projects seaward from the shelf (Broderick *et al.*, 2003; Figs 16 and 17A).

Seismic stratigraphy and facies distribution

Seaward of Santa Monica Canyon, there are two packets of high-amplitude basin-filling reflections, corresponding to the interval below the blue reflector and the interval from B to C. In addition, there is a near-surface levee wedge beside the fan valley, with sediment waves, between the F and H reflections (Fig. 16C).

Near the base of slope between the Dume and Santa Monica channels, just below the blue reflector, there are numerous small irregularities (Fig. 17A, north-west end), suggesting that small slope gullies may have been active at that time, but no such comparable features are found south-east of Santa Monica Canyon (Fig. 17A, south-east end). Santa Monica Canyon was wider and probably erosional at the blue reflection, but it has been partially filled by inner levee growth since that time.

DISCUSSION

Age model

Ages determined by radiocarbon dating for the top hundred metres of sea floor sediment at ODP Site 1015 are highly consistent (Fig. 3 inset), yielding reasonable sedimentation rates and coherent correlation to Site 893 on the basis of foraminiferal assemblages. Extrapolating the mean sedimentation rate from the seafloor to the D reflection yields an age estimate of 130 ka for the blue reflection.

Normark *et al.* (1998, fig. 8) showed that during the glacial interval from D to K, sediment was preferentially deposited on Hueneme fan mid-fan. In the Holocene, deposition took place preferentially in the basin, onlapping the edge of the mid-fan. Piper & Normark (2001) ascribed this change to the different flow properties of high-density hyperpycnal flows at lowstands compared with more turbulent flows initiated either by storms in submarine canyon heads or by transformation of slumps and debrisflows through hydraulic jumps during highstands. Applying this interpretation to line L490-125 (Fig. 6A), the interval from the seabed to B shows depositional patterns typical of lowstands, whereas the B to blue interval shows patterns characteristic of highstands. The interval from blue to brown is again characteristic of lowstand times. The age estimate of 130 ka for blue suggests that it correlates with the MIS 6 to 5 transgression at *ca* 127 ka and the blue to B interval corresponds to the MIS 5 highstand (Table 2).

Further extrapolation becomes more speculative, because in a tectonically active area the assumption of constant sedimentation rate becomes increasingly unlikely back through time. Brown probably represents the MIS 7 to 6 transition at *ca* 185 ka, with the brown to orange interval representing highstand deposition during MIS 7. Orange to green tentatively correlates with the MIS 8 lowstand and the transparent green to yellow interval may represent distal turbidites and hemipelagic deposition during the MIS 9 highstand. Blake (1991) recognized a regional onlap surface and unconformity that corresponds to the yellow horizon along a north–south seismic profile extending southward from coastal outcrops. His pick for the top of the Repetto Formation (within the late Pliocene) was 0·4 sec below yellow, with the overlying strata corresponding to the Pico Formation (late Pliocene to late Pleistocene age). Bohannon *et al.* (2004) interpreted the top of the Pico Formation at a level corresponding to reflector B in Santa Monica basin and to blue near Santa Monica Canyon.

An age model is also developed for the Santa Barbara Basin (Fig. 8) based on the published chronology of ODP Site 893. Linear extrapolation of sedimentation rates from ODP 893 suggests that the shallowest acoustically incoherent lens at the southern margin of the basin corresponds

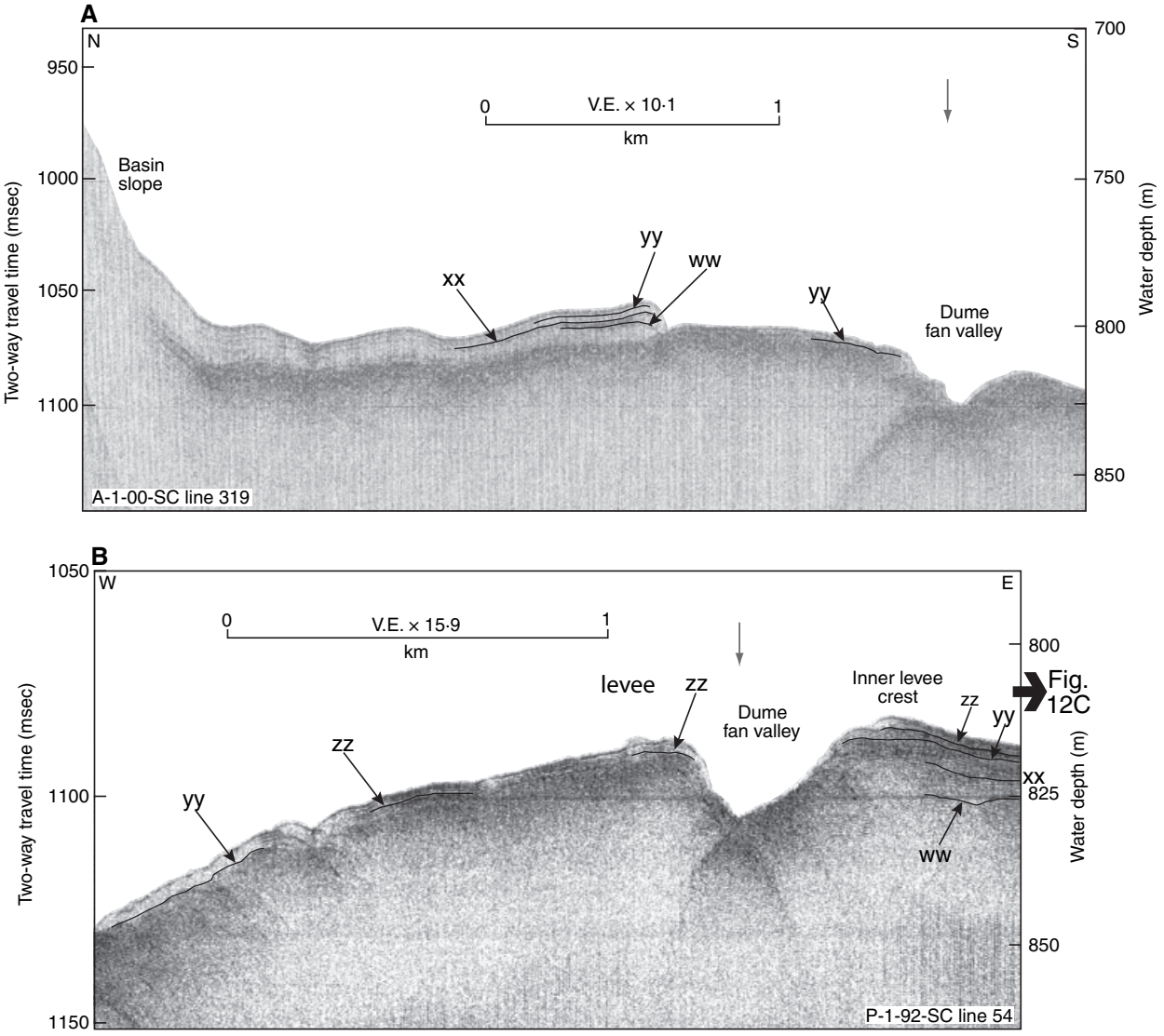

Fig. 12. Deep-tow boomer reflection profiles across the Dume Fan. Seismic-stratigraphic markers for the Dume Fan (xx, yy, etc.) are explained in text and Table 2. Position of core SMB3 (in italics) is projected onto the line of the profile. Profile locations shown in Fig. 2.

to MIS 10, the underlying mound to MIS 12 (continuing basinward as a reflection at 0·7 sec sub-bottom) and the basin-floor unconformity with onlap is likely of early Pleistocene or late Pliocene age. At the northern margin of the basin, erosional surfaces pass basinward into reflections that appear to mark the beginning of glacial stages.

Mugu, Dume and Santa Monica fans

Growth pattern and fan architecture

Like the Hueneme Fan, the Mugu Fan has been fed through delta-front channels of the Santa Clara delta. The growth of the Mugu Fan has been topographically constrained by a reverse fault just south-west of the foot of the continental slope, by the continental slope itself, and at times by mid-fan mounded deposition on the Hueneme Fan. Available seismic-reflection profiles (e.g. Fig. 9) suggest that at times mid-fan mounded deposition of sandy facies took place, commonly capped by a complex of small channels and levees. This facies succession is similar to that seen on the Hueneme Fan.

The Dume fan valley has progressively shifted north-westward during the late Pleistocene, in response to continuing deformation on the Dume fault and perhaps northward propagation of, or folding of basin-edge sediment related to, the San

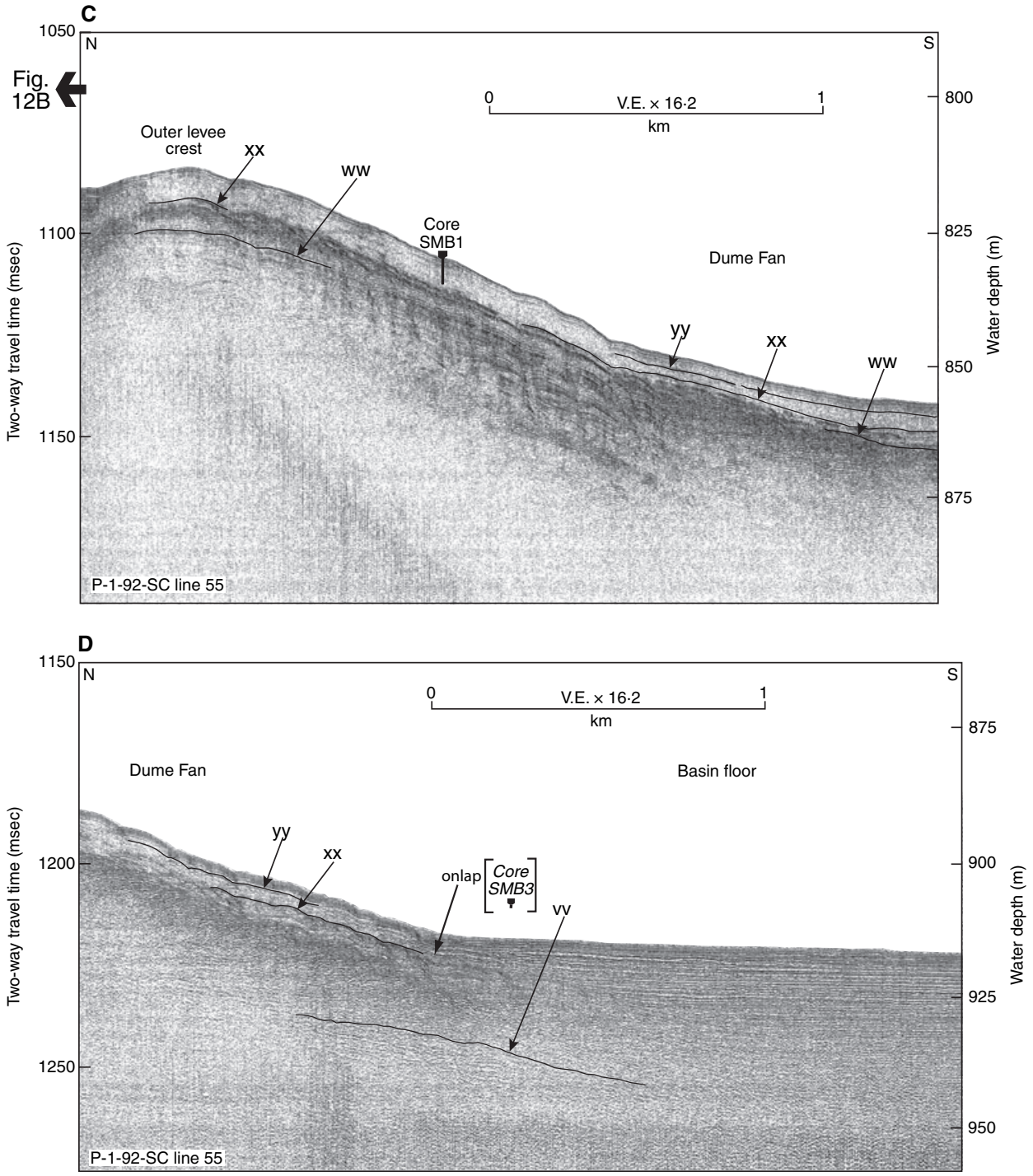

Fig. 12. (Continued).

Pedro Basin fault. The fan valley shows variable rates of growth of rather low levees, suggesting that sediment transported in turbidity currents was predominantly sandy. High-gradient coarse depositional lobes, with sandy or gravelly bedforms, extend <5 km from the termination of the fan valley (Figs 11B and 15) and there is no evidence that the Dume Fan has contributed much distal sediment to the Santa Monica Basin.

On the Santa Monica fan, the deposits for MIS 6 and 4 return parallel, high-amplitude reflections, similar to those of the distal Hueneme Fan, that appear to have been topographically constrained by active faulting at the southern end of the Santa

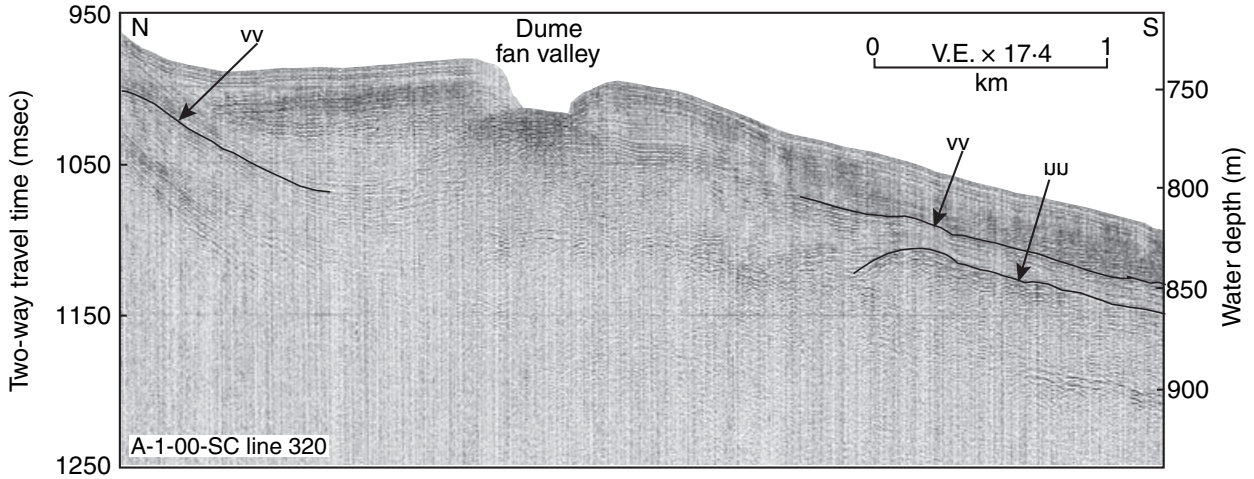

Fig. 13. Minisparker profile across the upper fan valley, Dume Fan. Profile location shown in Fig. 2.

Monica Basin. The MIS 2 deposits appear to consist principally of low levees with sediment waves along the Santa Monica fan valley, with more distal sediment indistinguishable from basin floor deposits in the southern Santa Monica Basin supplied from the Hueneme and Mugu fans. The fan was active only in the MIS 2, 4, and 6 lowstands because at higher stands of sea level, the Santa Monica canyon was stranded at the shelf edge.

Chronology of fan growth, links to sea level and sedimentation rates

The most pronounced deposition of coarse-grained mid-fan lobes on the Mugu fan in the last 125 000 years occurred in the interval just below reflection A (*ca* 110 ka), between B and C (approximately MIS 4) and just below J [after the first stage of rising sea level after the last glacial maximum (LGM)]. This pattern might be random and solely a consequence of shifting river-mouth positions on the Santa Clara delta, but it is interesting that all these intervals were times of intermediate sea level (Fig. 18) when Mugu Canyon would have been most active at the end of a littoral drift cell.

On the Dume Fan, there is no strong correlation with sea level of either the well-developed high-gradient lobes or of changes in fan-valley planform. Like the Mugu Fan, sandy lobe deposits are recognized during the MIS 5 highstand and larger lobes above C and above H either follow or are synchronous with large mid-fan lobes on the Mugu Fan. This sedimentation pattern may indicate that when the Santa Clara River discharged to the south-eastern part of the delta, supply of sediment to both the Mugu and Dume fans was enhanced.

The Santa Monica Fan received sediment only during extreme lowstands of sea level in MIS 2, 4 and 6. At other times, the Santa Monica shelf apparently was too wide to allow sediment to reach Santa Monica Canyon. Rather, Redondo Canyon would have been nourished, supplying sediment to San Pedro Basin (Fig. 1).

Sediment accumulation rates, coarse-grained sediment supply to the basin, and sea-level change

Intervals of rapid sediment accumulation can be identified from the seismic stratigraphy, both on the fans and on the basin floor (Fig. 19). In addition, intervals when coarse-grained sediment was deposited on fans are interpreted from acoustic facies (following the arguments of Normark *et al.*, 1998 and Piper *et al.*, 1999).

The most pronounced deposition of coarse-grained mid-fan lobes on the Mugu Fan in the last glacial cycle took place at an uncorrelated interval older than the B reflector (Fig. 9). This deposition may have prograded the fan sufficiently south-westward to an area where good seismic coverage is lacking, so that much of the identified younger fan growth is represented by the development of channel–levee systems. Coarse-grained mid-fan deposition is also recognized just above reflectors B, D and J.

On the Dume Fan, coarse-grained high-gradient lobes are recognized immediately above the teal and A reflectors on the southern margin of the fan (Fig. 15). A shift in fan valley position was

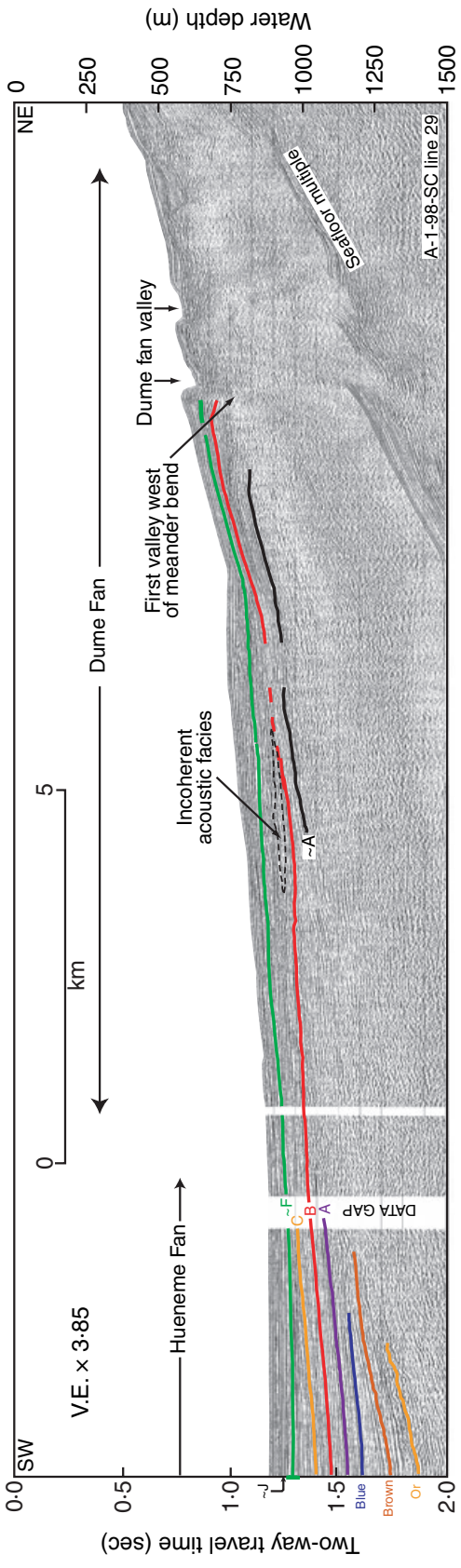

Fig. 14. Multichannel seismic-reflection profile A-1-99-SC Line 29 showing deeper stratigraphy of the Dume Fan and the correlation with deposits of the Hueneme Fan. See text for explanation. Profile location shown in Fig. 2.

followed by the development of a small coarse lobe a short distance above reflector B (Fig. 18). Coarse-grained lobes are also developed in the K to M interval (Fig. 11B).

Sandy growth phases of the Hueneme Fan resulted in deposition of thick, acoustically incoherent sediment wedges on the middle fan. The most important is between reflectors D to J (Fig. 7D). Earlier middle fan sand deposition is interpreted at the margins of the middle fan (e.g. Fig. 9) and acoustically incoherent lenses of coarse-grained sediment are found immediately above the teal, A and B reflectors. The package immediately above teal corresponds to a levee progradation phase illustrated in Fig. 7.

These various phases of coarse-grained mid-fan deposition are correlated to sea-level changes. Radiocarbon dating at ODP site 1015 allows the major mid-fan aggradational phase of the Hueneme Fan from D to J to be correlated with the extreme lowering of sea level to below −80 m at the end of MIS 3 and during MIS 2, using the sea-level curve of Lambeck & Chappell (2001) (Fig. 18). The older sandy phases at the fringe of the middle Hueneme fan are not dated precisely, but reasonably correlate with substantial drops in sea level during MIS 4, 5b and 5d. These three older sandy phases also correlate with deposition of sandy wedges on the Dume Fan. The main MIS 3-2 sea-level fall corresponds to an unconformity surface overlain by sandy wedges on the Dume Fan, but the volume of coarse sediment deposits and their rate of sedimentation is no greater than those dating from MIS 5 lowstand events (Fig. 19). The timing of coarse-grained mid-fan deposition on the Mugu Fan also correlates with sandy intervals on the other two fans, but rapid overbank deposition of levee deposits took place only above reflection J (Fig. 19).

The spatial and temporal variation in sedimentation rate within the Santa Monica Basin is summarized in Fig. 19. The distal Santa Monica Basin has a sedimentation rate of 2–3 mm yr^{-1} throughout much of the last 0·13 Ma, rising to 4·2 mm yr^{-1} during the MIS 2–3 extreme lowstand. Beneath the middle Hueneme Fan, rates were 1–1·5 mm yr^{-1} prior to the MIS 2–3 extreme lowstand, rising to 6 mm yr^{-1} during the last glacial maximum and decreasing to 1–2 mm yr^{-1} above reflection J. A similar pattern of much higher sedimentation rates during the last glacial maximum is found higher on the Hueneme Fan, with sedimentation rates up to 13 mm yr^{-1}. In contrast, on the middle Mugu Fan, the highest

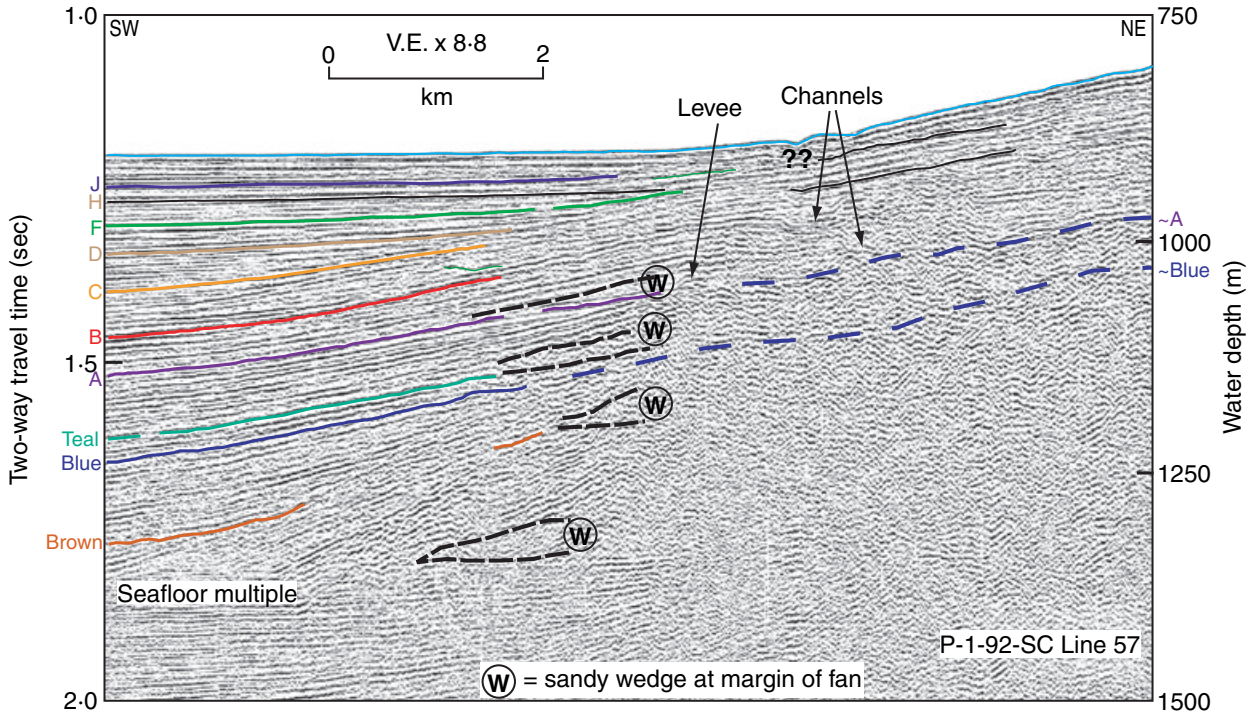

Fig. 15. Sleeve-gun seismic-reflection profile P-1-92-SC line 57 showing older channel and levee deposits on the Dume Fan and the toes of sandy wedges prograding into the basin. Profile location shown in Fig. 2.

accumulation rates are found in MIS 4 and in the post-LGM section above reflector J.

During the Holocene, river-mouth positions shifted autocyclically on the Santa Clara delta (Piper & Normark, 2001) and similar shifts probably took place during the Pleistocene. Nevertheless, at times of abrupt lowering of sea level in MIS 5d, 5b, 4 and 3-2, synchronous coarse-grained deposition took place on the Dume, Mugu and Hueneme fan systems. The lack of significant coarse-grained progradation Early in MIS 3, when sea level was substantially lower than during MIS 5 (Fig. 18), suggests that it was rapid lowering of sea level, rather than the absolute depth of sea level, that promoted coarse-grained sediment supply to the basin. This means that longshore drift can supply Santa Clara River sediment along the entire Hueneme–Mugu–Dume coastal system, but that at times of abrupt lowering of sea level, valley incision, an increase in river gradient, and cannibalization of older deltaic sediments resulted in pulses of coarse-grained deposition in the basin. The long-lived extreme lowstand of MIS 3-2, with sea level below −80 m, resulted in widespread sand deposition on the Hueneme Fan not only during the initial fall in sea level (between reflections D to F), but also throughout the lowstand. At the same time, evidence of rapid aggradation on the Mugu Fan is found only above reflection J (Fig. 9) and sandy lobes developed on the Dume Fan above reflection K (Fig. 11B). Thus during the extreme lowstand, deposition took place preferentially on the Hueneme Fan and it was only when sea level rose again to less than −80 m that there was important sediment deposition farther down the longshore drift system (Fig. 19). With steep river gradients as a result of the base-level lowering, it appears that the Santa Clara River flowed through an incised valley across its delta and discharged directly into the head of the Hueneme Canyon and fan valley during the last glacial maximum. The increase in sedimentation rate was much greater on the Hueneme Fan than on the distal basin floor, implying that much of the sediment was trapped on the fan, in contrast to most other times when sedimentation rate on the basin plain was similar to or greater than sedimentation rates on the fan. This dichotomy was previously recognized by Piper & Normark (2001) for the interval above reflector J. They interpreted the flows that deposited principally on the basin floor, resulting in thick sand beds there, as turbulent flows initiated by canyon-head currents or transformation of debrisflows. The flows that deposit principally on the fan, including thick sandy lobes, were interpreted as hyperpycnal flows from flood stages of the Santa Clara River and deposited mostly thin-bedded sand units on

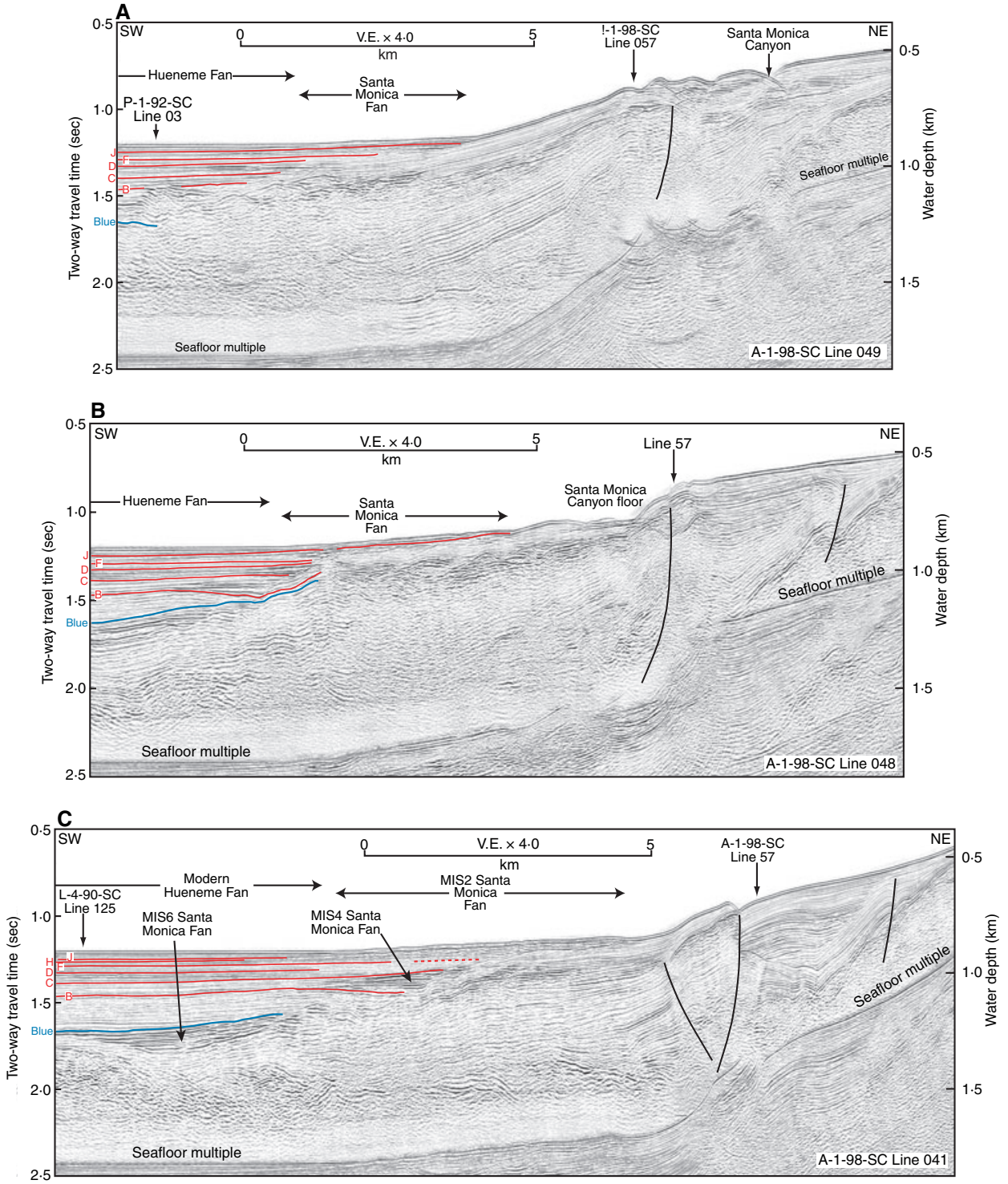

Fig. 16. Three parallel multichannel seismic-reflection profiles across the lower basin slope and Santa Monica Canyon. The Santa Monica Fan deposits extend only a few kilometres into the basin-plain area of the Hueneme Fan. Faults are associated with the San Pedro Basin fault zone (Fisher *et al.*, 2003). Profile locations shown in Fig. 2.

the basin floor. The predominance of such flows during the extreme MIS 3-2 lowstand would be expected, given that the river would have discharged directly into deep water, with an incised valley across the shelf. Only as sea level rose again did a sandy delta with multiple distributaries form, allowing the nourishment of the Mugu and Dume systems and reducing the importance of

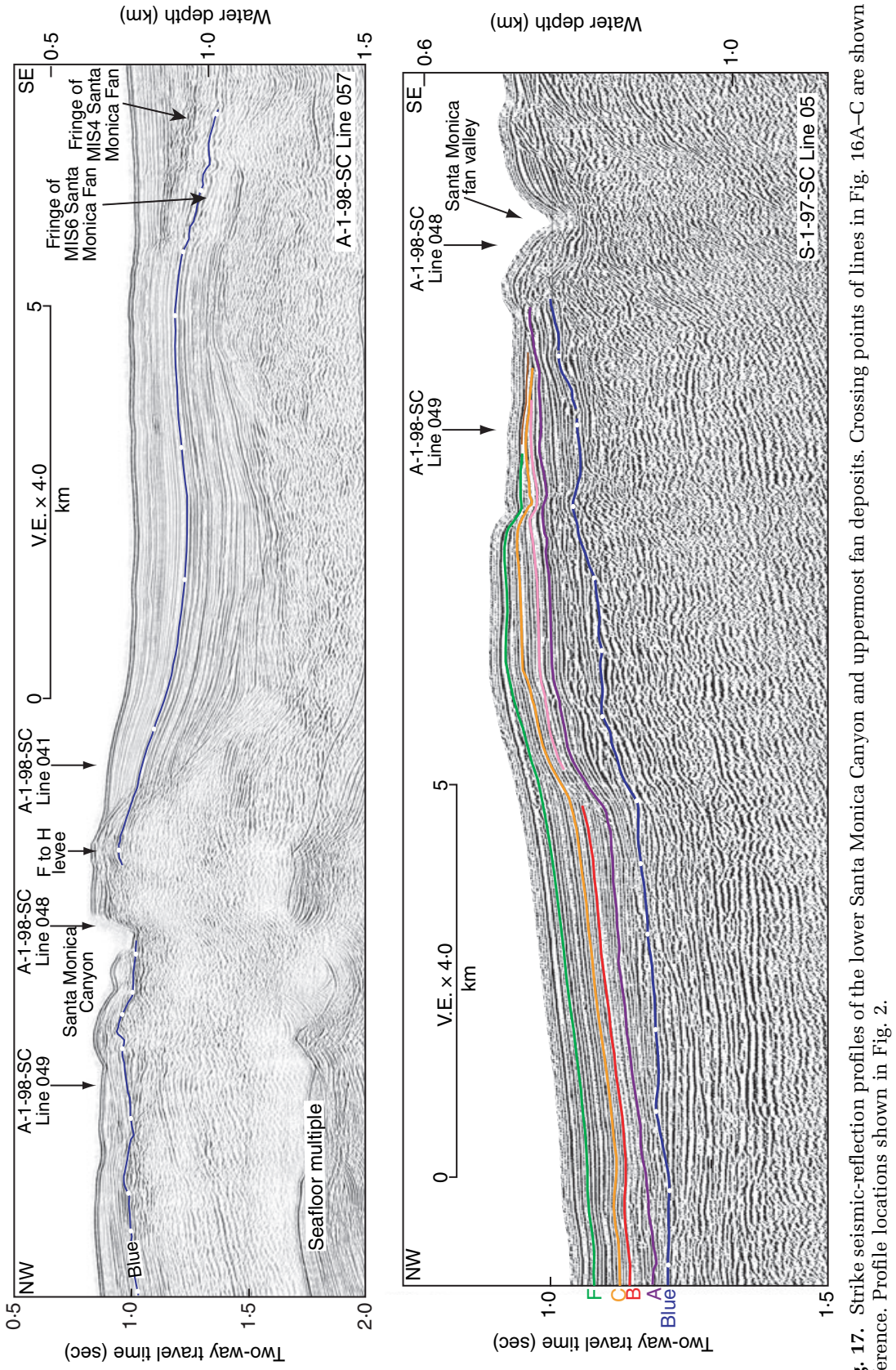

Fig. 17. Strike seismic-reflection profiles of the lower Santa Monica Canyon and uppermost fan deposits. Crossing points of lines in Fig. 16A–C are shown for reference. Profile locations shown in Fig. 2.

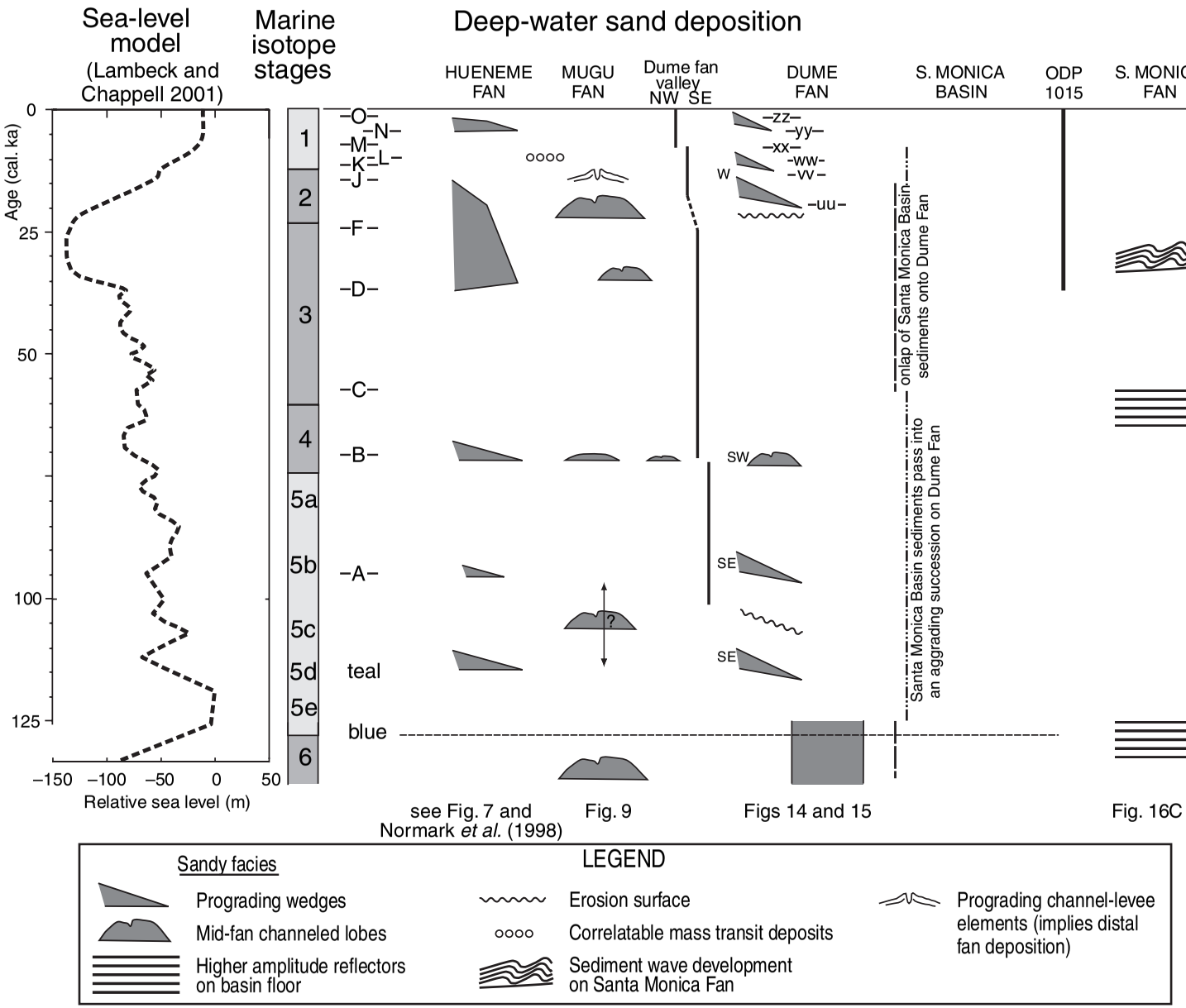

Fig. 18. Age model for key reflectors showing timing of principal coarse-sediment supply to the Hueneme, Mugu and Dume fans. Figure references for each fan near the bottom of this schematic summary show where the interpretation is best illustrated. Sea-level curve from Lambeck and Chappell (2001).

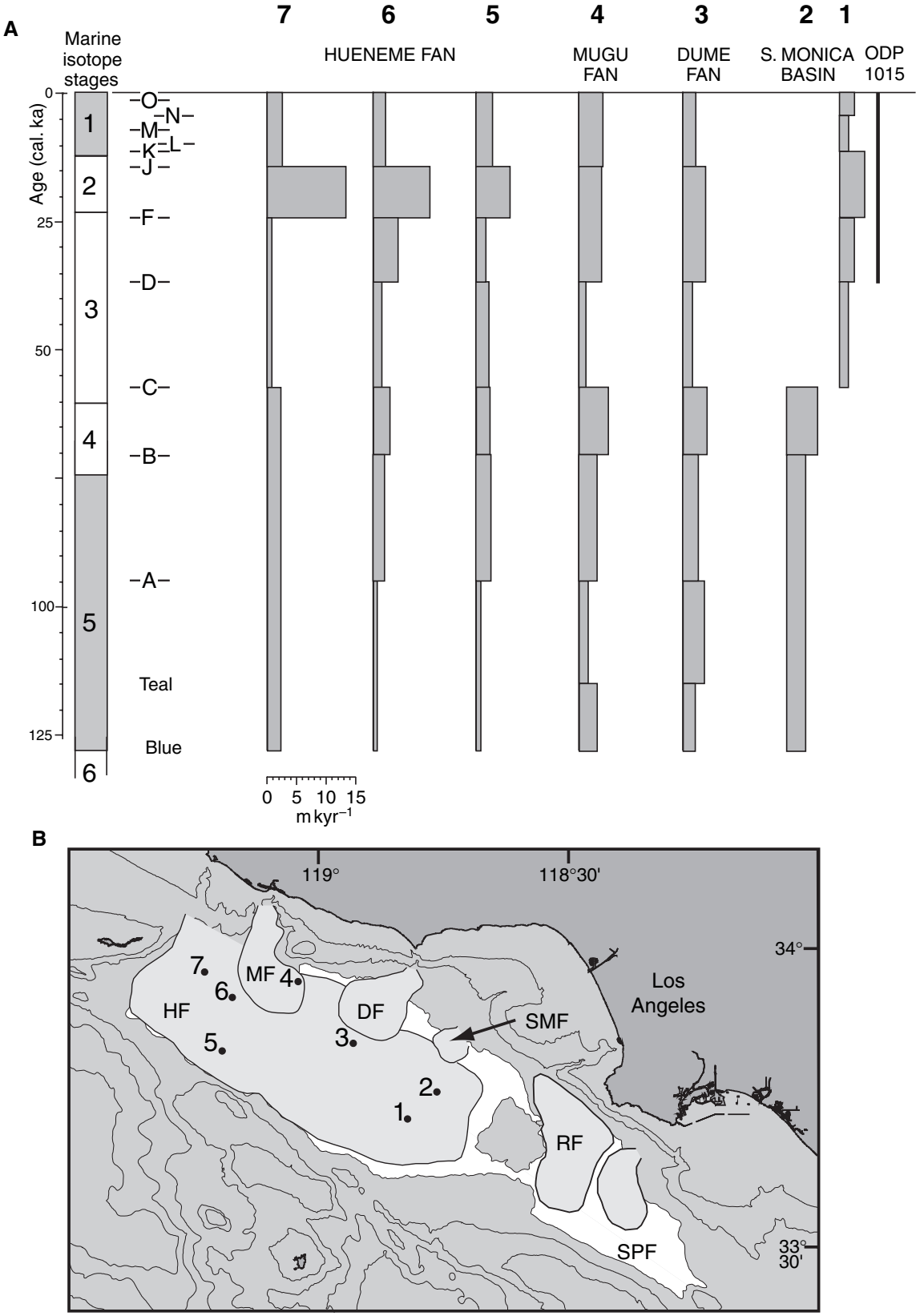

Fig. 19. Variation in sedimentation rate in the Santa Monica Basin since the blue reflection (end of MIS 6, 127 ka). Based on age model in Fig. 18 and thicknesses measured from seismic-reflection profiles shown in Figs 6A, 7, 8 and 14 (assuming uniform $V = 1600$ m sec^{-1}).

hyperpycnal flow. There may be an analogy with the Santa Monica Fan, which received sediment only during extreme lowstands of sea level during MIS 2, 4 and 6. At other times, the Santa Monica shelf would have been too wide to allow sediment to reach Santa Monica Canyon. Rather, Redondo Canyon would have been nourished, supplying sediment to San Pedro Basin (Fig. 1).

Large-scale evolution of Santa Monica Basin – the role of tectonics

The principal source of sediment to the Santa Monica Basin is the Santa Clara River, whose delta is located on the northern side of the Malibu Coast–Santa Cruz Island fault zone that separates the Santa Monica from the Santa Barbara Basin (Figs 1 and 20). The age model developed above implies that the yellow reflector, marking a prominent onlap surface and a change in sedimentation style in the Santa Monica Basin, dates from about MIS 10. Prior to that, the mean sedimentation rate for the late Pliocene Pico Formation and early Quaternary was of the order of 200 m Myr^{-1} based on the picks of Blake (1991), suggesting that either deposition was in shallow water and limited by accommodation or that the Santa Clara River discharged into the Santa Barbara Basin.

In the Santa Barbara Basin, evidence of deep basinal turbidite sedimentation is much earlier than in the Santa Monica Basin, extending back perhaps to the base of the Pleistocene (Fig. 20). The prominent lobe deposits at the eastern end of the basin date from MIS 10 and 12, and earlier in the Pleistocene, sandy fan sediment from an uncertain source was trapped in the northern graben. Following MIS 10, sedimentation appears to have been similar to that recorded from MIS 1-6 by ODP 893. Subsidence of the Anacapa ridge may have allowed the Santa Clara–Ventura rivers to discharge southward with subsidence creating accommodation in the Santa Monica Basin. The MIS 6 fan in the Santa Monica Basin has grown across subsiding earlier Quaternary stratified sediment, probably a shelf succession along the faulted basin margin, whereas the MIS 8 fan is on the basin floor south-east of that fault block (Fig. 6).

CONCLUSIONS

This study traces the evolution of a small sandy turbidite system, fed by a 'dirty', high- sediment-

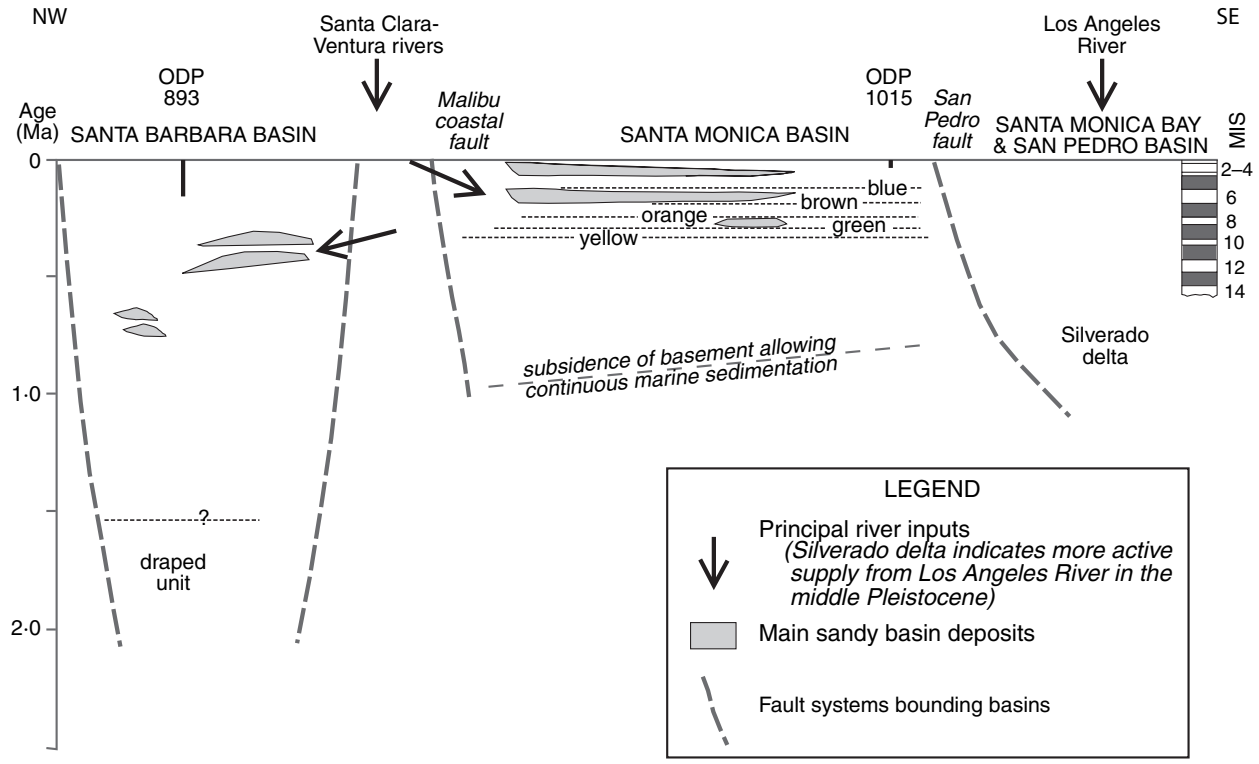

Fig. 20. Age model for the Quaternary tectonic evolution of the Santa Monica and Santa Barbara basins and resulting changes in sediment supply, shown on a highly schematic north-west to south-east section. For further explanation, see text.

discharge river, that has developed in a subsiding transpressional basin since MIS 10 (0·3 Ma). Local tectonics controlled the discharge of the Santa Clara River, switching coarse terrigenous sediment from the eastern Santa Barbara Basin to the north-western Santa Monica Basin as the Anacapa ridge subsided. A detailed age model back to *ca* 36 ka has been obtained from radiocarbon dating of foraminifera from ODP Site 1015 and has been extrapolated back over the last glacial cycle. Over that time span, sedimentation has been strongly influenced by sea-level change. Sedimentation rates in the distal part of Santa Monica Basin averaged 2–3 mm yr^{-1}, with small increases at times of extreme sea-level lowstand. Coarser-grained mid-fan lobes prograded into the basin as the Hueneme, Mugu and Dume fans grew rapidly at times of rapid sea-level fall. Such pulses of coarse-grained sediment resulted from river channel incision and delta cannibalisation. During the extreme lowstand of the last glacial maximum, sediment delivery was concentrated on the Hueneme Fan, at mean rates of 6 mm yr^{-1} on the mid- and upper fan, implying that the incised Santa Clara River delivered sediment directly to the head of the Hueneme Canyon and fan valley as hyperpycnal flows. During the MIS 2 to 1 transgression, relatively high rates of sedimentation occurred on the Mugu and Dume fans, as a result of distributary switching and southward littoral drift on the Santa Clara delta providing nourishment to these fan systems. The style and distribution of turbidite sedimentation is thus a consequence of two main factors that are both controlled by sea level: the rate of supply of coarse sediment (greatest during incision and cannibalization) and the style of initiation of turbidity currents, influencing whether sand is deposited principally on the mid-fan or transported to the basin plain. These two factors appear more important than the absolute position of sea level.

ACKNOWLEDGEMENTS

We thank Mary McGann, Thian Hundert and Shawna Weir-Murphy for assistance with foraminifera picking and Denise Brushett for help in compiling the log in Fig. 3. Calvin Campbell and Christina Gutmacher provided digital navigation files for use with the seismic-reflection data loaded into seismic processing systems at the USGS and GSC and also helped with scanning archived paper records. The manuscript was improved thanks to reviews by David Mosher, Jon Warrick, Helen Gibbons, Lawrence Amy and Peter Haughton. GSC contribution number – 2005318.

REFERENCES

Bard, E., Rosteck, F. and **Ménot-Combes, G.** (2004) A better radiocarbon clock. *Science*, **303,** 178–179.

Blake, G.H. (1991) Review of the Neogene biostratigraphy and stratigraphy of the Los Angeles Basin and implications for basin evolution. In: *Active Margin Basins* (Ed. K.T. Biddle), *AAPG Mem.*, **52,** 135–184.

Bohannon, R.G., Gardner, J.V. and **Sliter, R.W.** (2004) Holocene to Pliocene tectonic evolution of the region offshore of the Los Angeles urban corridor, southern California. *Tectonics*, **23,** TC1016, doi:10·1029/2003TC00150, 34 p.

Broderick, K., Sorlien, C., Luyendyk, B., Kamerling, M., Sliter, R., Fisher, M. and **Normark, B.** (2003) Blind thrust faulting and shelf-slope deformation in eastern Santa Monica Bay, California. 2003 SCEC Ann. Sci. Meet. Proc. Abstr., **XIII,** 70.

Christensen, C.J., Gorsline, D.S., Hammond, D.W. and **Lund, S.P.** (1994) Non-annual laminations and expansion of anoxic basin floor conditions in Santa Monica Basin, California Borderland, over the past four centuries. *Mar. Geol.*, **116,** 399–418.

Crouch, J.K. and **Suppe, J.** (1993) Late Cenozoic tectonic evolution of the Los Angeles basin and inner California borderland: A model for core complex-like crustal extension. *Geol. Soc. Am. Bull.*, **103,** 1415–1434.

Dahlen, M.Z., Osborne, R.H. and **Gorsline, D.S.** (1990) Late Quaternary history of the Ventura mainland shelf, California. *Mar. Geol.*, **94,** 317–340.

Edwards, B.D., Field, M.F. and **Kenyon, N.H.** (1996) Morphology of small submarine fans, inner California Continental Borderland. In: *Geology of the United States' Seafloor: The View from GLORIA* (Eds J.V. Gardner, M.E. Field and D.G. Twichell), pp. 235–249. Cambridge University Press, Cambridge.

Fisher, M.A., Normark, W.R., Bohannon, R.G., Sliter, R.W. and **Calvert, A.J.** (2003) Geology of the continental margin beneath Santa Monica Bay, Southern California, from seismic-reflection data. *Bull. Seismol. Soc. Am.*, **93,** 1955–1983.

Fukushima, Y., Parker, G. and **Pantin, H.M.** (1985) Prediction of ignitive turbidity currents in Scripps submarine canyon. *Mar. Geol*, **67,** 55–81.

Gardner, J.V. and **Dartnell, P.** (2002) Multibeam Mapping of the Los Angeles, California Margin. U.S. Geol. Surv. Open-File Rep. OF02-162.

Gorsline, D.S. (1996) Depositional events in Santa Monica Basin, California Borderland, over the past five centuries. *Sed. Geol.*, **104,** 73–88.

Kennett, J.P. and **Venz, K.** (1995) Late Quaternary climatically related planktonic foraminiferal assemblage changes: Hole 893A, Santa Barbara Basin, California. In: *Proceedings ODP Scientific Results* (Eds J.P. Kennett, J.G. Baldauf and M. Lyle), vol. 146:2, pp. 281–293. Ocean Drilling Program, College Station, TX.

Kienast, S.S. and **McKay, J.L.** (2001) Sea surface temperatures in the subarctic northeast Pacific reflect millennial-scale climate oscillations during the last 16 kyrs. *Geophys. Res. Lett.*, **28,** 1563–1566.

Klitgord, K.D. and **Brocher, T.** (1996) Oblique-slip deformation in the San Pedro Basin offshore Southern California region, EOS. *Trans. Am. Geophys. Union*, **77,** p. F737.

Kovanen, D.J. and **Easterbrook, D.J.** (2002) Paleodeviations of radiocarbon marine reservoir values for the Northeast Pacific. *Geology*, **30,** 243–246.

Lambeck, K. and **Chappell, J.** (2001) Sea level change through the last glacial cycle. *Science*, **292,** 679–686.

Lyle, M., Gallaway, P. and **Mix, A.C.** (1995) W9406 and EW9504 Site Surveys of the California Margin Proposed Drilling Sites, Leg. 167. Tech. Rep. BSU CGISS 95-12, Boise State University, Boise, ID.

Mulder, T. and **Syvitski, J.P.M.** (1995) Turbidity currents generated at mouths of rivers during exceptional discharges to the world oceans. *J. Geol.*, **103,** 285–299.

Nardin, T.R. (1983) Late Quaternary depositional systems and sea level change - Santa Monica and San Pedro Basins, California Continental Borderland. *AAPG Bull.*, **67,** 1104–1124.

Nardin, T., Osborne, R.H., Bottjer, D.J. and **Schneidermann, R.C.** (1981) Holocene sea-level curves for Santa Monica shelf, California continental borderland. *Science*, **213,** 331–333.

NOAA (1998) *NOS Hydrographic Survey Data, U.S. Coastal Waters*: Boulder, CO, World Data Center for Marine Geology and Geophysics, Data Announcement 00-MGG-05 (http://www.ngdc.noaa.gov/mgg/fliers/00mgg05.html).

Normark, W.R. and **McGann, M.** (2004) Late Quaternary deposition in the Inner Basins of the California Continental Borderland: Part A. Santa Monica Basin. US Geol. Surv. Scientific Invest. Rep. 2004-5183, 21 p. (http://pubs.usgs.gov/sir/2004/5183/).

Normark, W.R. and **Piper, D.J.W.** (1998) Preliminary evaluation of recent movement on structures within the Santa Monica Basin, offshore southern California. *US Geol. Surv., Open-File Rep.* 98-518, 60 p.

Normark, W.R., Hein, J.R., Powell, C.L. II, Lorenson, T.D., Lee, H.J. and **Edwards, B.D.** (2003) Methane Hydrate Recovered From A Mud Volcano in Santa Monica Basin, Offshore Southern California. *Eos Transactions American Geophysical Union*, **84**(46), Fall Meet. Suppl., Abstract OS51B–0855.

Normark, W.R., Piper, D.J.W. and **Hiscott, R.N.** (1998) Sea level effects on the depositional architecture of the Hueneme and associated submarine fan systems, Santa Monica Basin, California. *Sedimentology*, **45,** 3–70.

Piper, D.J.W. and **Normark, W.R.** (2001) Sandy fans – from Amazon to Hueneme and beyond. *AAPG Bull.*, **85,** 1407–1438.

Piper, D.J.W., Hiscott, R.N. and **Normark, W.R.** (1999) Outcrop-scale acoustic facies analysis and latest Quaternary development of Hueneme and Dume submarine fans, offshore California. *Sedimentology*, **46,** 47–78.

Reynolds, S. (1987) A recent turbidity current event, Hueneme fan, California: reconstruction of flow properties. *Sedimentology*, **34,** 129–137.

Schwalbach, J.R., Edwards, B.D. and **Gorsline, D.S.** (1996) Contemporary channel-levee systems in active borderland basin plains, California Continental Borderland. *Sed. Geol.*, **104,** 53–72.

Shipboard Scientific Party (1997) Site 1015. In: *Proceedings of ODP, Initial Reports* (Eds M. Lyle, I. Koizumi, C. Richter *et al.*), vol. 167, pp. 223–237. Ocean Drilling Program, College Station, TX.

Sorlien, C., Broderick, K., Kamerling, M., Fisher, M., Normark, W.R., Sliter, R. and **Seeber, L.** (2003) Structure and kinematics beneath Santa Monica Bay, California. AAPG (Pacific Section) Conf. Program Abstr., May 2003, p. 90.

Southon, J.R., Nelson, D.E. and **Vogel, J.S.** (1990) A record of past ocean-atmosphere radiocarbon differences from the Northeast Pacific. *Paleoceanography*, **5,** 197–206.

Stuiver, M., Reimer, P.J., Bard, E., Beck, J.W., Burr, G.S., Hughen, K.A., Kromer, B., McCormac, G., van der Plicht, J. and **Spurk, M.** (1998) INTCAL98 radiocarbon age calibration, 24,000–0 cal BP. *Radiocarbon*, **40,** 1041–1083.

Toggweiler, J.R., Dixon, K. and **Bryan, K.** (1989) Simulations of radiocarbon in a coarse-resolution world ocean model 1. Steady state prebomb distributions. *J. Geophys. Res.*, **94,** 8217–8242.

Vedder, J.G. (1987) Regional geology and petroleum potential of the Southern California Borderland. In: *Geology and Resource Potential of the Continental Margin of Western North America and Adjacent Ocean Basins - Beaufort Sea to Baja California* (Eds D.W. Scholl, A. Grantz and J.G. Vedder), *Circum-Pacific Coun. Energy Mineral Resour. Earth Sci. Ser.*, Houston, TX, **6,** 403–447.

Warrick, J.A. and **Milliman, J.D.** (2003) Hyperpycnal sediment discharge from semiarid southern California rivers— Implications for coastal sediment budgets. *Geology*, **31,** 781–784.

Wright, T.L. (1991) Structural geology and tectonic evolution of the Los Angeles Basin, California. In: *Active Margin Basins* (Ed. K.T. Biddle), *AAPG Mem.*, **52,** 35–134.

Manuscript received 5 August 2005; revision accepted 5 April 2006